International Journal of Concrete Structures and Materials

RESEARCH

Open Access

# Numerical Simulation and Fatigue Analysis of the Grout Layer Replacement for Horizontal Joint of Wind Turbine Prestressed Concrete Tower

Ziwei Wang[1], Dongping Huang[2], Minjuan He[1,3] and Zheng Li[1,3*]

**Abstract**

There are many engineering applications of prestressed concrete tower as the wind turbine support structure, and the concrete tower has the advantages of applicability and economy with good prospects. This paper proposes a grout layer replacement scheme for the problem of grout missing in the horizontal joint of concrete tower segments, and conducts a series of numerical simulation and fatigue analysis. The simulation results show that, for the case of grout missing, there is an obvious stress unevenness in the local area of severe grout missing. The concrete compressive stress decreases, tensile stress increases, tensile damage zone develops, and steel rebars stress increases, which can lead to local concrete cracking and blocks falling. For the case of grout filling and replacement completion, using no expansion grout for repair makes little contributions to the recovery of concrete stress, while using slight expansion grout can restore the concrete local stress to an even state. The fatigue analysis results show that, for the case of grout missing, the fatigue damage factors greatly exceed the limit, indicating a short fatigue life and the potential risk of local failure. For the case of grout filling and replacement completion, using no expansion grout cannot decrease fatigue damage, while using slight expansion grout can decrease fatigue damage and improve fatigue life. This paper provides the investigation into the effectiveness of grout layer replacement for horizontal joint, and the presented results can provide technical supports for the analysis and solution of grout missing problems.

**Keywords** Wind turbine tower, Prestressed concrete, Horizontal joint, Grout layer, Finite element modeling

## 1 Introduction

Wind energy is renewable and can effectively meet current and future energy demand of the society. Wind turbine is the device that converts wind energy into electricity, which can be cost-effective and sustainable (Hernandez-Estrada et al., 2021). At present, the wind energy market is vast, with a global new installed capacity of 116.6 GW and a total global installed capacity of 1021 GW in 2023. China's new installed capacity in that year accounted for 65% of the world's total, including 69 GW for onshore and 6.3 GW for offshore (GWEC, 2024). With the construction and development of onshore wind turbines in China, trying to use of wind resources in areas with low wind speed and high shear rate has become the main development direction, which puts higher demands on blade length, hub height, tower height, etc. Wind turbine towers over 140 meters have gradually become mainstream. At this

Journal information: ISSN 1976-0485 / eISSN 2234-1315.

*Correspondence:
Zheng Li
zhengli@tongji.edu.cn
[1] Department of Structural Engineering, College of Civil Engineering, Tongji University, Shanghai 200092, China
[2] Tongji Architectural Design (Group) Co., Ltd, Shanghai 200092, China
[3] State Key Laboratory of Disaster Reduction in Civil Engineering, Tongji University, Shanghai 200092, China

time, the use of concrete tower or steel-concrete hybrid tower has outstanding economic advantages (Grünberg & Göhlmann, 2013; Cheng et al., 2024).

Concrete tower can be mainly divided into two forms, which named cast-in-place tower and prefabricated tower (von der Haar & Marx, 2015). Prefabricated concrete tower have the advantages of short construction time and high industrialization level, and is the mainstream of engineering applications. Prefabricated concrete tower normally requires the post tensioned prestressed steel strands to ensure structural integrity, hence it is also called prestressed concrete tower. In 2005, the National Renewable Energy Laboratory (NREL) proposed a design for prestressed concrete towers and conducted detailed structural analysis (LaNier, 2005). Since then, many scholars conducted comprehensive research on prestressed concrete towers. Lotfy (2012) proposed a tower with a triangular cross-section and conducted design calculations and finite element analysis. Alvarez-Anton et al. (2016) designed a composite tower with a quadrilateral cross-section, while Peggar (2017) designed a tower with an octagonal cross-section, they aimed to save the concrete form. Ma et al. (2015) designed the quasi-static test on a scaled concrete tower model with an octagonal cross-section and made finite element simulations. The results can verify the rationality of the design. Ren et al. (2023) proposed the steel-concrete composite tower segment of sandwich-like section, and conducted axial compression test and numerical simulation. While Chen et al. (2024a) further proposed the steel-concrete composite section with corrugated steel plates, and also conducted static tests and numerical simulations. However, currently in China, ordinary circular cross-section is the mainstream for practical engineering applications of the concrete towers.

Due to production and transportation limitations, the prefabricated concrete tower needs to be segmented, with horizontal joints and vertical joints (Fig. 1a, b). The horizontal and vertical joints of the prefabricated concrete tower are usually the weakest parts of the structure. There are two forms of connection, the wet joint and the dry joint, for both horizontal and vertical joints. The wet joint with on-site grouting has good structural integrity, but the construction time will be long. The dry joint has high construction efficiency, but the structural integrity will be weakened. For vertical joint, bolt connections can be used generally. For horizontal joint, depending on the flatness of the concrete surface, it can be directly connected without additional measures or connected through a leveling layer. In China, commonly, the horizontal joint is connected through a grout layer, which made by epoxy resin or cement mortar (Fig. 1c).

Using dry horizontal joints greatly improves construction efficiency, but in extreme situations, there is a risk of horizontal joint opening and contact detachment. Kang et al. (2019), Klein et al. (2022), Fürll et al. (2024), Chen et al. (2024b) studied the problem of joint opening of the horizontal joint and the section bearing capacity under detachment, but they did not take the grout layer into account. Jonscher et al. (2023) noticed the concrete surface waviness of the dry horizontal joint, and they mainly studied the influence of imperfections on structural mode shapes through experiments. Song et al. (2016) focused on the mechanical performance of the horizontal joint, paying attention to the simulation of the grout layer, but did not consider the possible defects of the layer. The standards, IEC 61400-1 (2019), IEC 61400-6 (2020) and DNVGL-ST-0126 (2016), are important references

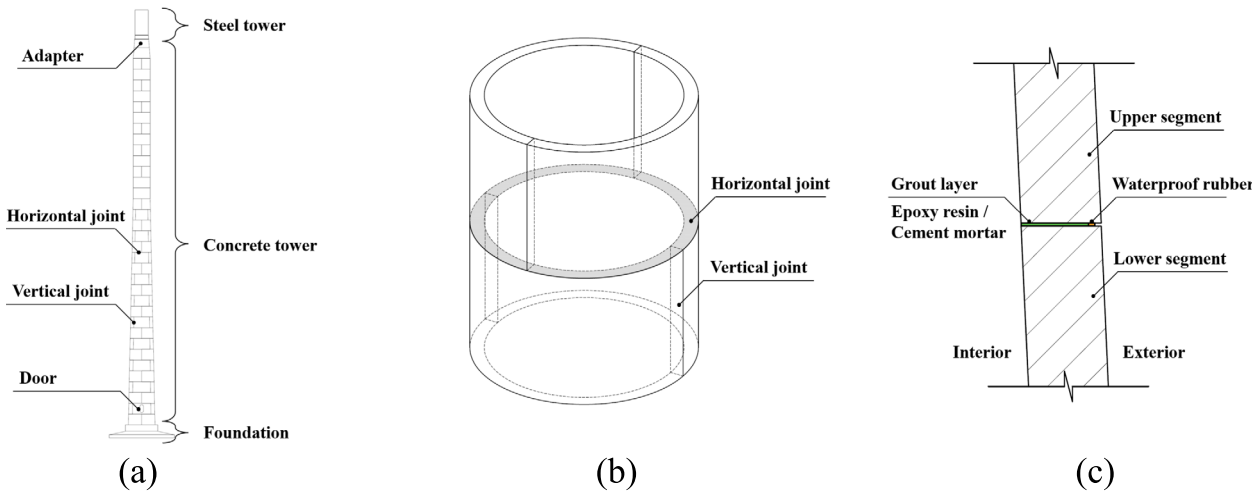


**Fig. 1** **a** Wind turbine steel-concrete hybrid tower, **b** concrete segments with joints, **c** horizontal joint with grout layer

for wind turbine tower design. According to the standards, the mechanical verification of the horizontal joints for the prestressed concrete tower is necessary and the geometry imperfections should be considered. Nevertheless, there is a lack of research on the missing of grout layer and the possible negative influence on the concrete tower. Meanwhile, no relevant research reports on grout layer replacement and repair have been found yet.

This paper focus on the wind turbine prestressed concrete tower, and bases on the problem of grout layer missing in the horizontal joints of a practical engineering project. A replacement repair scheme is proposed, and two possible properties of the repair grout are considered. ABAQUS is used for finite element simulation to obtain the mechanical response of the concrete tower structure during the replacement repair process. Based on the simulation results, further fatigue analysis of the local concrete section is carried out. The conclusions of this paper are expected to provide references for the design of grout layer repair scheme and the research of the similar structure in the future.

## 2 Numerical Simulation

### 2.1 Overview

The steel-concrete hybrid towers were used in a practical project, with the prestressed concrete tower height of 104 meters. During operation, obvious concrete cracking and blocks falling were observed near the horizontal joints (Fig. 2). It was speculated to be caused by uneven grout layers, and probe detection was carried out accordingly. Taking the horizonal joint between the first and second segments as an example, where the tower door is, the detection result is shown in Fig. 3. Detection points were arranged along the circular direction, and were drawn on the straight coordinate axis. The tower wall thickness is 250 mm. The outside 40 mm is the waterproof rubber and the cavity, and the inside 210 mm is the grout layer where the missing may occur. The figure represents the depth of probe detection point, which indicates the depth of missing grout layer at the point.

To solve the problem of grout layer missing in the horizontal joint, this paper proposes a scheme of local replacement repair for the grout layer (Fig. 4). The specific steps are as follows: (1) Inject grout from the outside to fill the missing part of grout layer; (2) Completely

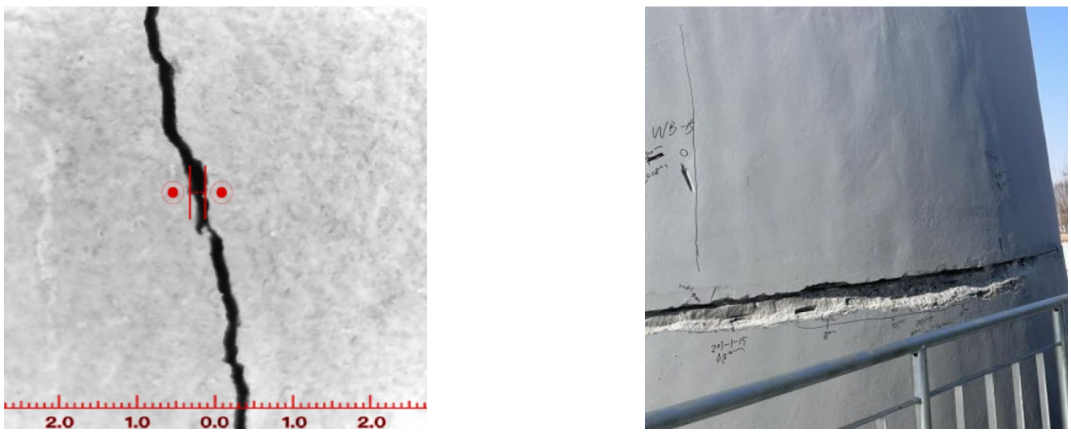


**Fig. 2** **a** Concrete cracking, **b** concrete blocks falling

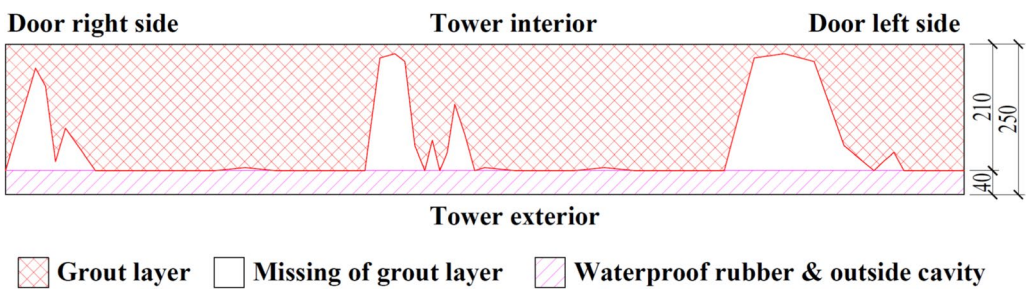


**Fig. 3** Result of probe detection

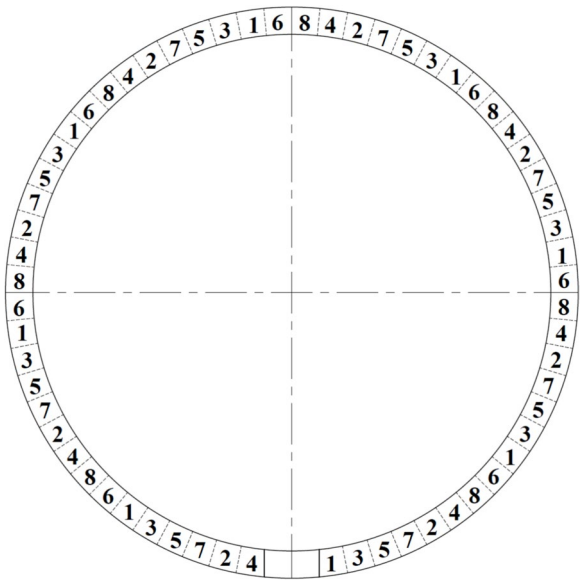

**Fig. 4** The scheme of local replacement repair

chisel off Area One; (3) Fill Area One with grout and chisel off Area Two; (4) Follow the above steps to chisel and fill Area One to Eight in sequence; (5) Complete the local replacement repair and the entire layer can bear the load. The advantages of using this scheme of local replacement repair are as follows: (1) There is no need to unload or dismantle the upper part of the tower; (2) It can reduce the layer unevenness by taking one-time grouting method (i.e., only take the step (1) mentioned above).

### 2.2 Model Description

ABAQUS is commonly used for fine simulation of wind turbine concrete towers (Cao et al., 2020; Lin et al., 2023; Li et al., 2024). This paper establishes a finite element model in ABAQUS based on actual engineering drawings. Concrete tower is founded by the solid, where the first and second segments are the research objects while the foundation and the third and fourth segments serve as boundary conditions, considering a segment thickness of 250 mm and a segment height of 3640 mm (Fig. 5a).

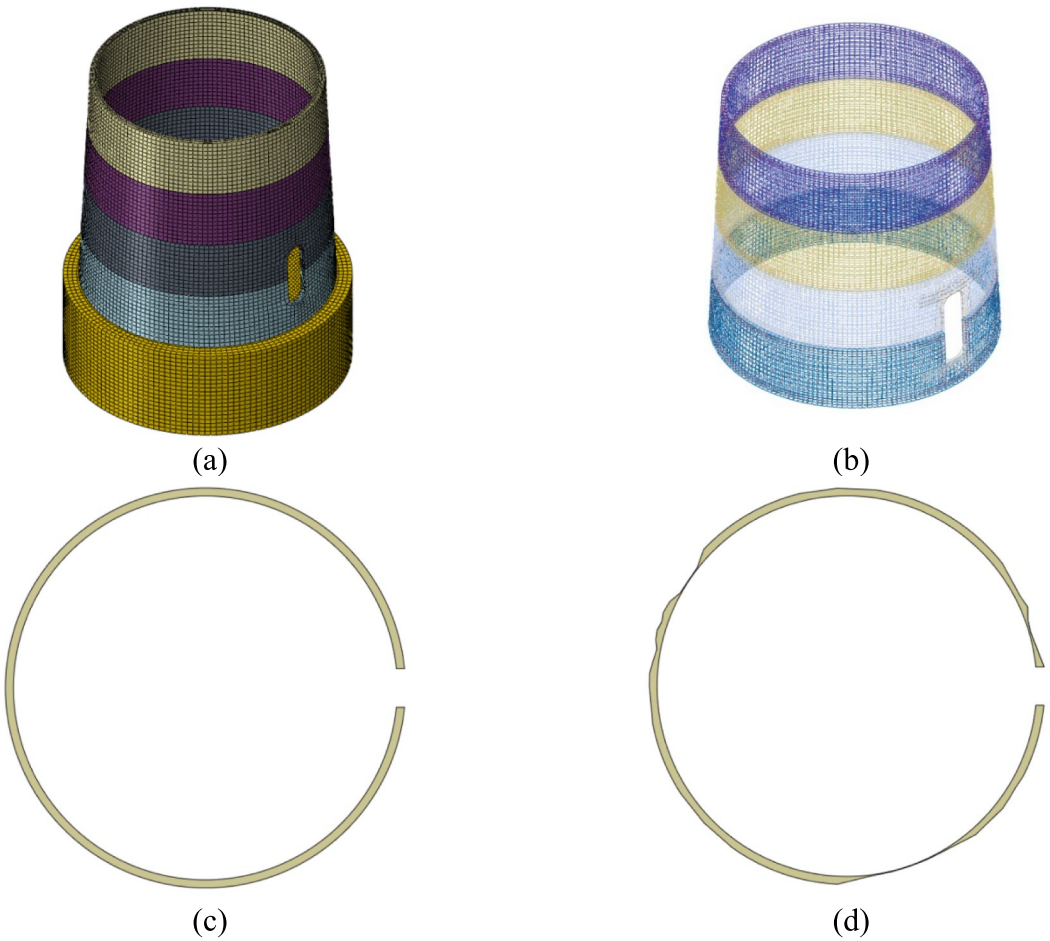


**Fig. 5** Finite element model of **a** concrete tower, **b** rebar, **c** grout layer without missing, **d** grout layer with missing

Steel rebars are founded by the line, considering radial, circumferential, longitudinal, and door opening additional rebars (Fig. 5b). Grout layers are founded by the solid, considering a thickness of 3 mm and a width of 210 mm. Ideally, the grout layer have an intact circular cross-section without any missing (Fig. 5c). Actually, in the initial simulation step, the grout layer will be considered the missing based on the detection result (Fig. 5d).

The basic control size of the finite elements is 200 mm. Six elements are set along the thickness direction to densify the local mesh. The model has a total of 200,000 elements, approximately.

As shown in Fig. 6, the bottom of the foundation is constrained with all degrees of freedom as fixed. Tie constraints are set between the tower segments and the grout layer to simulate the bonding of the grout. The steel rebars are embedded into the concrete tower segments. A reference point is set at the center of the upper surface of the top concrete segment, and it is coupling with the surface.

### 2.3 Model Variables

The tower is made of C70 concrete. Referring to GB 50010-2010 (2015) *Code for Design of Concrete Structures* Appendix C, the concrete damage plastic model (CDPM) is adopted. The compressive and tensile strengths are taken as standard values of 44.5 MPa and 2.99 MPa, respectively. Constant values of 30°, 0.1, 1.16 and 0.67 are used for dilation angle ($\psi$), flow potential eccentricity ($e$), the ratio of the second stress invariant on the tensile meridian to that on the compressive meridian ($K_c$) and the ratio of the compressive strength under biaxial loading to uniaxial compressive strength ($f_{b0}/f_c'$), respectively

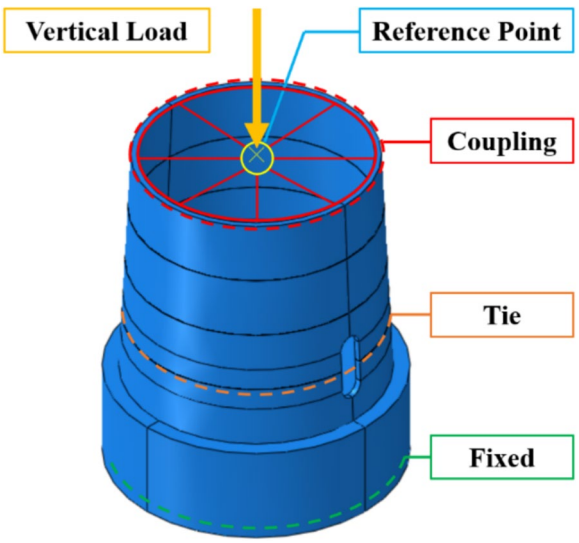


**Fig. 6** The interactions and boundary conditions of the model

(Tao et al., 2013). The definition of damage factors is based on the energy method (Sidoroff, 1981). The steel rebar is made of HRB400 material, and adopts an ideal elastic-plastic model with a yield strength of 400 MPa. The grout layer is made of epoxy resin or cement mortar. According to the studies (Iwamoto et al., 2010; Pang et al., 2018; Elruby & Nakhla, 2019), epoxy resin performed elasticity in both tension and compression before failure. In addition, according to the product manual, its compressive strength exceeds 100 MPa and its tensile strength exceeds 5 MPa ensuring that failure occurs in concrete. Therefore, an ideal elastic model can be used for this simulation. The main material parameters are shown in Table 1, where $E$ is the elastic modulus and $\mu$ is the Poisson's ratio.

For the replacement of grout layer, two models are considered: (1) Model One: using epoxy resin for grouting, which will solidify without expansion and fill the grout layer cavity precisely without initial stress and strain. So, the local area will not immediately participate in bearing load; (2) Model Two: using cement mortar for grouting, which will solidify with certain expansion, or adopting some measures (such as lifting) to promote stress redistribution during replacement process. So, after grouting, the local area will immediately participate in bearing load (the expansibility of cement mortar is adjustable in the practical application, assuming that its expansibility can restore local deformation to the ideal state). The two models are completely identical, except for the different technical methods used in simulating the grout layer replacement. The model change method in ABAQUS is used for simulating the replacement process. The elements of grout missing areas are deactivated, and in the steps of replacement the elements of grout filling areas will be reactivated. Differently, in Model One the elements will be reactivated without strain, and in Model Two the elements will be reactivated with strain. In this way, it can simulate the two situations mentioned above.

### 2.4 Simulation Cases

The simulation in this paper involves 12 cases, namely: Case Ideal, Case Missing, Case Fixing, Case Replacement One to Eight, and Case Completion. The specific descriptions of the cases are shown in Table 2.

**Table 1** Material parameters

| Component | Material | Element type | $E$ (MPa) | $\mu$ |
|---|---|---|---|---|
| Concrete | C70 | C3D8R | 37000 | 0.2 |
| Steel rebar | HRB400 | T3D2 | 200000 | 0.3 |
| Grout | Epoxy resin or cement mortar | C3D8R | 8000 | 0.2 |

**Table 2** Simulation cases

| Name | Description |
|---|---|
| Case ideal | The grout layer is ideal without missing (cf. Fig. 5c) |
| Case missing | The grout layer is defective with missing (cf. Fig. 5d) |
| Case filling | Fill the missing areas of the grout layer with grout |
| Case replacement one | Chisel off area one (cf. Fig. 4) |
| Case replacement two | Fill area one with grout and chisel off area two (cf. Fig. 4) |
| Case replacement three | Fill area two with grout and chisel off area three (cf. Fig. 4) |
| Case replacement four | Fill area three with grout and chisel off area four (cf. Fig. 4) |
| Case replacement five | Fill area four with grout and chisel off area five (cf. Fig. 4) |
| Case replacement six | Fill area five with grout and chisel off area six (cf. Fig. 4) |
| Case replacement seven | Fill area six with grout and chisel off area seven (cf. Fig. 4) |
| Case replacement eight | Fill area seven with grout and chisel off area eight (cf. Fig. 4) |
| Case completion | Fill area eight with grout (cf. Fig. 4) |

The tower prestressing system consists of 30 bundles of steel strands, each consisting of 11 steel strands with a nominal diameter of 15.2 mm. Each strand has a nominal cross-section area of 140 $mm^2$ and a controlling tensile stress of 1340 MPa. The calculated equivalent prestressing load is 61,908 kN. The representative gravity value of the upper concrete tower is 17,880 kN. Therefore, in all cases, the load is a vertical downward equivalent concentrated force of 79,788 kN applied at the reference point (cf. Fig. 6).

## 3 Simulation Results

### 3.1 Validation

The outer diameter of the bottom of the circular concrete tower first segment is 10,700 mm and the inner diameter is 10,200 mm. The top outer diameter of the second segment is 10,226 mm and the inner diameter is 9726 mm. As stated in Sect. 2.4, the load is a downward concentrated force of 79,788 kN. Therefore, the theoretically calculated vertical compressive stress of the two concrete segments is between 9.72 and 10.18 MPa.

The finite element model will be validated by the vertical stress of concrete for Case Ideal. As shown in Fig. 7a, the vertical stress contour (in MPa) of the first and second tower segments is presented, with negative values indicating compression. The maximum value is set to − 8 MPa, the minimum value is set to − 12 MPa, and the values between them are displayed in color. It can be seen that in most area the vertical stress of the concrete segments is between 8 to 12 MPa in compression. And only in the area near the horizontal joint and near the door, the stress value is not within the range. The stress deviation near the horizontal joint is due to the fact that the surfaces are not in full contact, and there is a small outer cavity (cf. Fig. 1c). This results in the lower stress on the outer elements and the higher stress on the

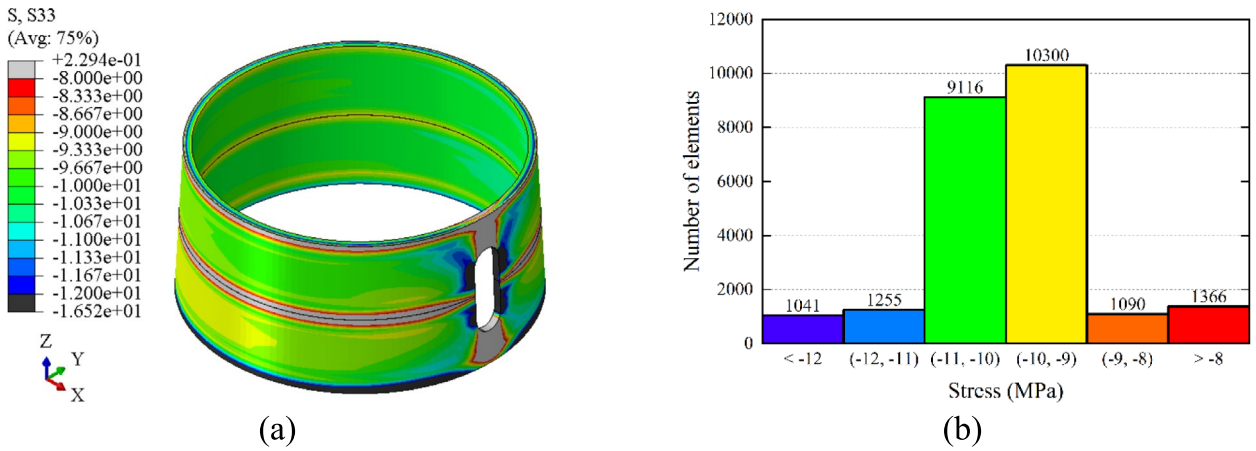


**Fig. 7** **a** The vertical stress of concrete segments for case ideal, **b** the distribution of vertical stress of finite elements

inner elements. The tower door is a significant weakening of the cross-section, and it is reasonable to have higher tensile and compressive stresses nearby. As shown in Fig. 7b, it is a bar chart of the distribution of vertical stress of elements. It can be seen that the vertical stress values of most of the elements (80 %) are between 9 to 11 MPa in compression and are in good agreement with the theoretical values (9.72 to 10.18 MPa), which can validate the effectiveness of the model.

### 3.2 Concrete stress Analysis

#### *3.2.1 Model One*

As shown in Fig. 8, the minimum principal stress contours (in MPa) of the first and second tower segments

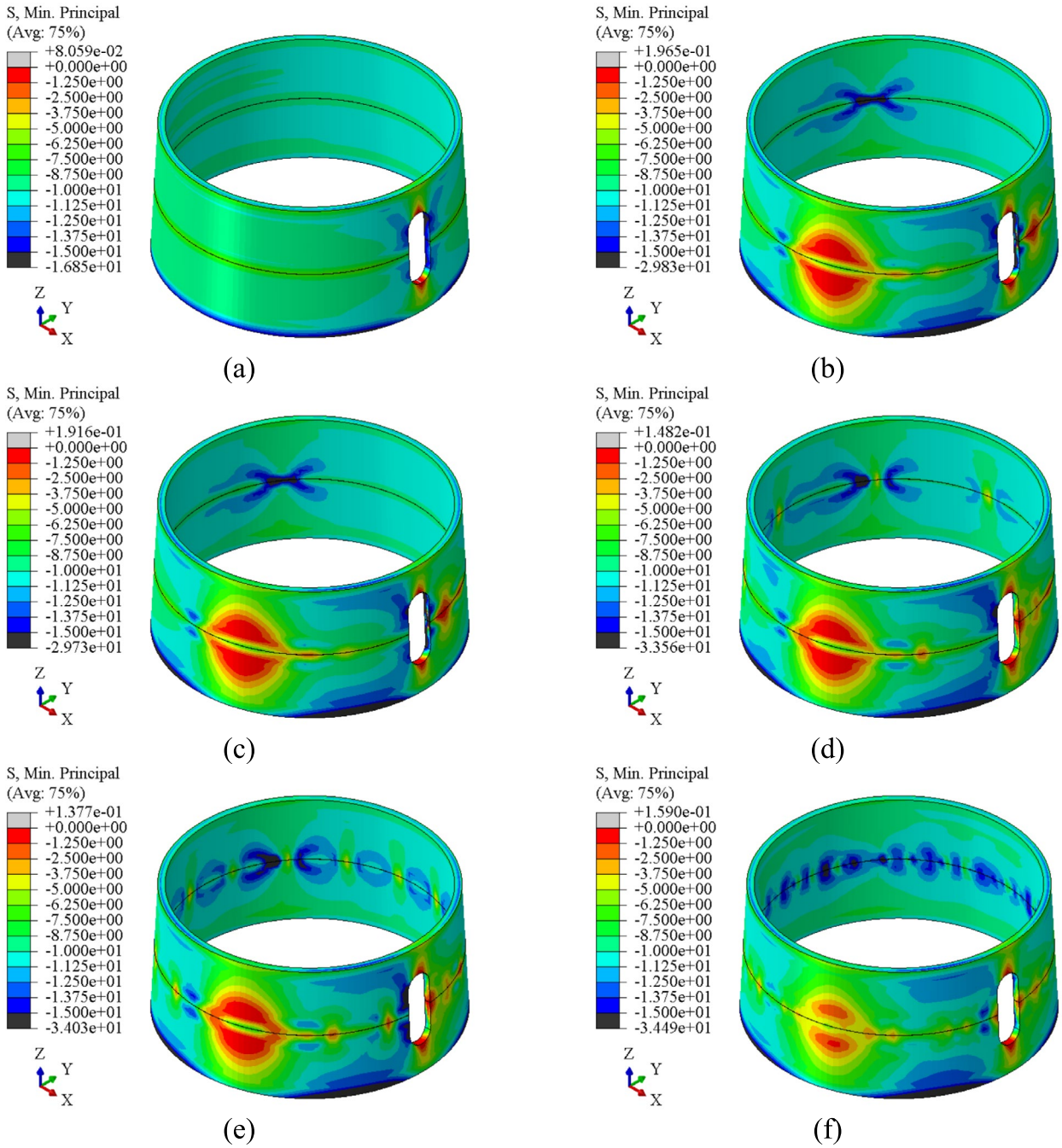


**Fig. 8** The minimum principal stress of concrete segments of model one for **a** case ideal, **b** case missing, **c** case filling, **d** case replacement one, **e** case replacement two, **f** case completion

of Model One (no expansion grout) are presented, with negative values indicating compression. The contours of Case Replacement Two to Eight have some similarities and will be omitted (the same below). The maximum value of the contour is set to zero, and the regions above that will be gray. The minimum value of the contour is set to − 15 MPa, and the regions below that will be black.

For Case Ideal, the overall compressive stress distribution of the concrete segments is even, with most of the compressive stress between 8 to 12 MPa (Fig. 8a), which is consistent with the theoretical calculation value. According to the detection result (cf. Fig. 3), there was a noticeable missing of grout on both sides of the door. For Case Missing, the stress distribution at those positions tends to be uneven, with the compressive stress value of the concrete above and below the grout missing cavity significantly decreasing, and beside the grout missing cavity increasing (Fig. 8b). For Case Filling, because of filling with no expansion grout, the local areas do not immediately participate in bearing load, so there is no significant difference in the stress distribution from Case Missing (Fig. 8c). For Case Replacement One, the grout in Area One is removed by chiseling, and the compressive stress distribution of the concrete near the area tends to be uneven accordingly (Fig. 8d). For Case Replacement Two, the grout in Area Two is removed and the grout in Area One is filled. The removed area will lose its load-bearing capacity, while the filled grout will not participate in bearing load, immediately. The compressive stress distribution of the concrete near Area Two tends to be uneven, and that near Area One will not recover soon (Fig. 8e). For Case Completion, due to the local replacement repair process, the entire section can participate in bearing load together, and the problem of local low or high compressive stress can be slightly alleviated, but it cannot restore the stress distribution of the concrete segments to the Case Ideal (Fig. 8f).

As shown in Fig. 9, the maximum principal stress contours (in MPa) of the first and second tower segments of Model One (no expansion grout) are presented, with positive values indicating tension. The minimum value of the contour is set to zero, and the regions below that will be black. The maximum value of the contour is set to 2.4 MPa, and the regions above that will be gray.

For Case Ideal, the overall tensile stress distribution of the concrete segments is even and the value is relatively low (Fig. 9a). For Case Missing, the tensile stress value of concrete near the grout missing positions increases obviously (Fig. 9b). For Case Filling, as the grout will not immediately participate in bearing load after filling, there is no significant difference between the stress distribution from Case Missing (Fig. 9c). For Case Replacement One, the tensile stress value of the concrete near Area One increases accordingly (Fig. 9d). For Case Replacement Two, the tensile stress value of the concrete near Area Two increases, while that near Area One will not recover (Fig. 9e). For Case Completion, the problem of local high tensile stress can be alleviated to some extent, but it cannot restore the stress distribution of the concrete segments to the Case Ideal (Fig. 9f).

#### *3.2.2 Model Two*

As shown in Fig. 10, the minimum principal stress contours (in MPa) of the first and second tower segments of Model Two (slight expansion grout) are presented, with negative values indicating compression. The maximum value of the contour is set to zero, and the regions above that will be gray. The minimum value of the contour is set to − 15 MPa, and the regions below that will be black.

There is no difference in the results between Model One and Model Two for Case Ideal and Case Missing (Fig. 8a, b), so they will be omitted. For Case Filling, assuming that the grout can be filled densely and can immediately participate in bearing load, the local and overall compressive stress distribution of the concrete segments tends to be even visibly (Fig. 10a). For Case Replacement One, the compressive stress distribution of the concrete near Area One tends to be uneven accordingly (Fig. 10b). For Case Replacement Two, the compressive stress distribution of the concrete near Area Two tends to be uneven, while that near Area One recovers (Fig. 10c). For Case Completion, the uneven compressive stress of the tower segments can be significantly alleviated, and the stress distribution can be mostly restored to the Case Ideal (Fig. 10d).

As shown in Fig. 11, the maximum principal stress contours (in MPa) of the first and second tower segments of Model Two (slight expansion grout) are presented, with positive values indicating tension. The minimum value of the contour is set to zero, and the regions below that will be black. The maximum value of the contour is set to 2.4 MPa, and the regions above that will be gray.

There is no difference in the results between Model One and Model Two for Case Ideal and Case Missing (Fig. 9a, b). For Case Filling, the local and overall tensile stress distribution of the concrete segments tends to be even (Fig. 11a). For Case Replacement One, the tensile stress value of the concrete near Area One increases accordingly (Fig. 11b). For Case Replacement Two, the tensile stress value of the concrete near Area Two increases, while that near Area One recovers (Fig. 11c). For Case Completion, the uneven tensile stress of the tower can be alleviated to some extent, but due to irreversible local tensile damage to the concrete during the replacement process, the tensile stress distribution cannot be restored to the Case Ideal (Fig. 11d).

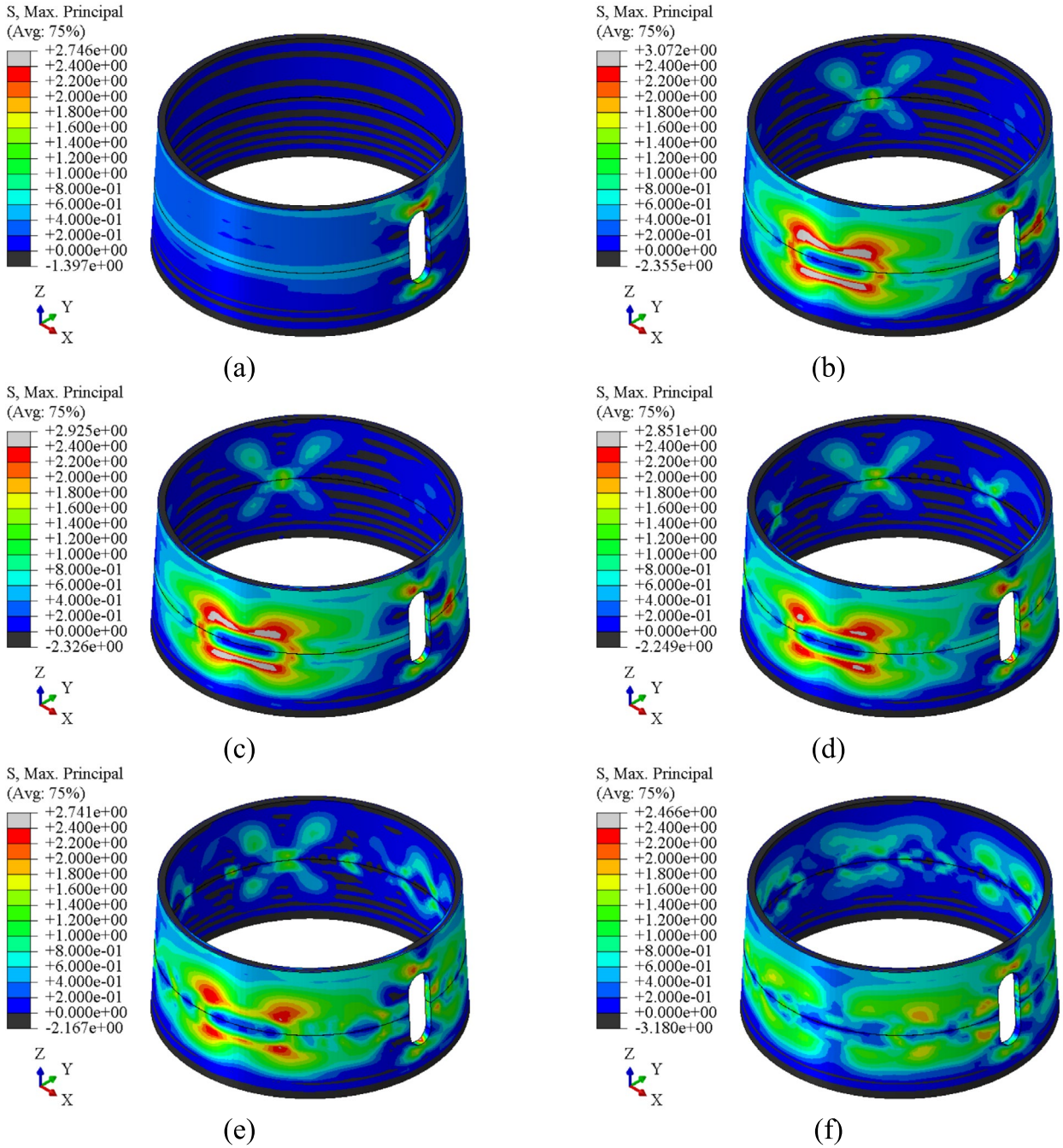


**Fig. 9** The maximum principal stress of concrete segments of model one for **a** case ideal, **b** case missing, **c** case filling, **d** case replacement one, **e** case replacement two, **f** case completion

### 3.3 Concrete Damage Analysis

When the tensile or compressive stress of concrete exceeds a certain limit, it is considered that irreversible material damage has occurred, and the elastic modulus and ultimate stress will decrease. The variables of the concrete damage model are as defined in Sect. 2.3. In this analysis, the tensile damage of concrete is prominent particularly, while the compressive damage of concrete is not significant, so it will be omitted.

#### *3.3.1 Model One*

As shown in Fig. 12, the tensile damage contours of the first and second segments of Model One (no expansion

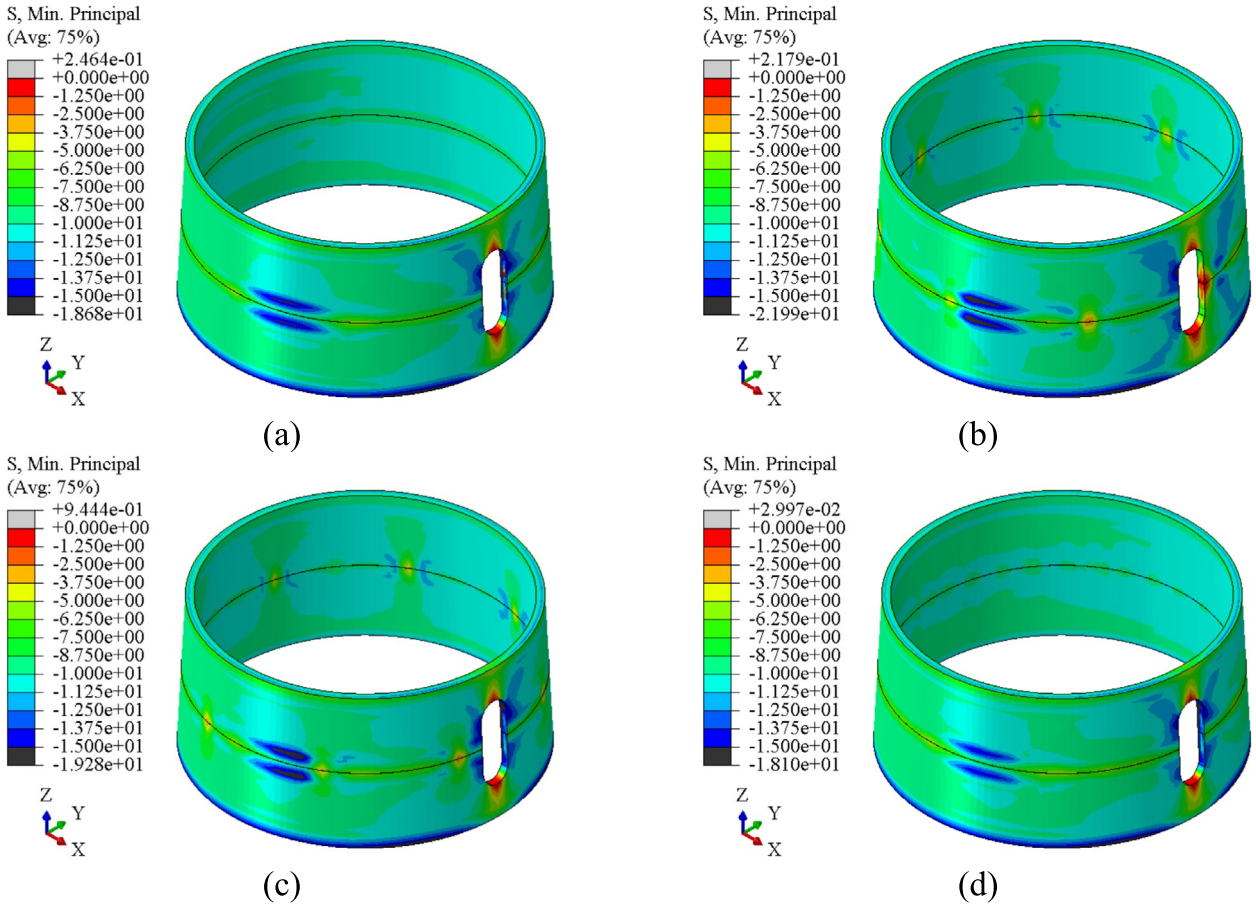


**Fig. 10** The minimum principal stress of concrete segments of model two for **a** case filling, **b** case replacement one, **c** case replacement two, **d** case completion

grout) are presented. A value of zero indicates no damage, while value of one indicates complete damage.

For Case Ideal, the concrete is almost undamaged, with local damage occurring only above and below the door (Fig. 12a). For Case Missing and Filling, there are significant concrete tensile damage areas near the obvious grout missing position (Fig. 12b, c). For Case Replacement One and Two, the concrete near the chiseled area also developed into a local tensile damage zone (Fig. 12d, e). For Case Completion, after the processes of Case Replacement One to Eight, there are obvious tensile damage areas around the concrete contact surface, but the range of damage areas is not so large (Fig. 12f).

#### *3.3.2 Model Two*

As shown in Fig. 13, the tensile damage contours of the first and second segments of Model Two (slight expansion grout) are presented. A value of zero indicates no damage, while value of one indicates complete damage.

Since the concrete damage is irreversible, the development of tensile damage of Model Two is similar to that of Model One (cf. Fig. 12), as described in Sect. 3.2.1.

### 3.4 Rebar Stress Analysis

#### *3.4.1 Model One*

As shown in Fig. 14, the Mises stress contours (in MPa) of the steel rebars inside the first and second tower segments of Model One (no expansion grout) are presented. For easy observation, the maximum value of the contour is set to 100 MPa, and the regions above that will be gray.

For Case Ideal, the stress distribution of the rebars is almost even, and there is a significant stress concentration near the door, which is reasonable (Fig. 14a). For Case Missing, the stress distribution of the rebars near the grout missing position is noticeably uneven, with the stress value of rebars near the horizontal joint increasing and a little away from the joint decreasing (Fig. 14b). For Case Filling, due to the fact that the grout will not immediately participate in the bearing load, there is no significant difference in the stress distribution from Case

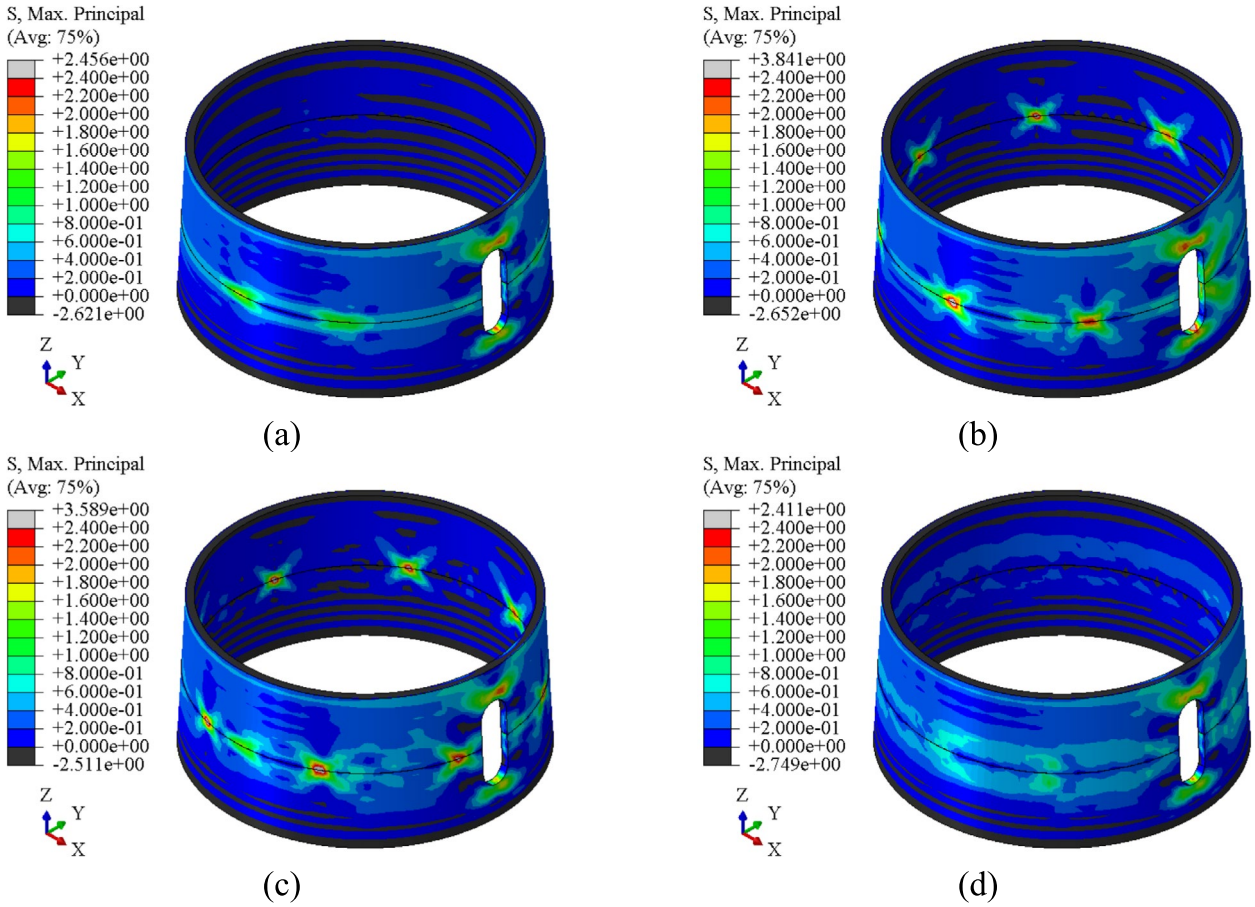


**Fig. 11** The maximum principal stress of concrete segments of model two for **a** case filling, **b** case replacement one, **c** case replacement two, **d** case completion

Missing (Fig. 14c). For Case Replacement One and Two, the stress distribution of the rebars near the chiseled area tends to be uneven accordingly (Fig. 14d, e). For Case Completion, referring to the results of concrete tensile stress (cf. Fig. 9f) and tensile damage (cf. Fig. 12f), the high Mises stress areas of the rebars corresponds to the high tensile stress areas and obvious tensile damage areas of concrete (Fig. 14f).

#### *3.4.2 Model Two*

As shown in Fig. 15, the Mises stress contours (in MPa) of the steel rebars inside the first and second tower segments of Model Two (slight expansion grout) are presented. For easy observation, the maximum value of the contour is set to 100 MPa, and the regions above that will be gray.

The Mises stress variation of rebars in Model Two is basically similar to that in Model One, as described in Sect. 3.3.1. The high Mises stress areas of the rebars corresponds to the high tensile stress areas (cf. Fig. 11) and obvious tensile damage areas (cf. Fig. 13) of concrete. The repair of the grout layer makes the stress of the rebars tend to be even, but it will not fully restore to the Case Ideal (Fig. 15d).

### 3.5 Contact Stress Analysis

In order to study the stress of the horizontal contact surface of tower segments, the vertical stress (i.e., S33 in ABAQUS) of the top elements of the first tower segment is extracted, and the vertical stress of the bottom elements of the second tower segment is basically consistent with it. As shown in Fig. 16, the Element 1 to 6 in the legend of later figures means the six elements along the wall thickness, with Element 1 being the outermost one and Element 6 being the innermost one. The Average means the arithmetic average of the values in Element 2 to 6, since Element 1 is located on the outside of the waterproof rubber (cf. Fig. 1c), where there is no grout layer to transfer the load, while Element 2 to 6 have the grout layer to transfer the load. The X-axis of the later figures unfolds the circular cross-section into a straight line, with the leftmost

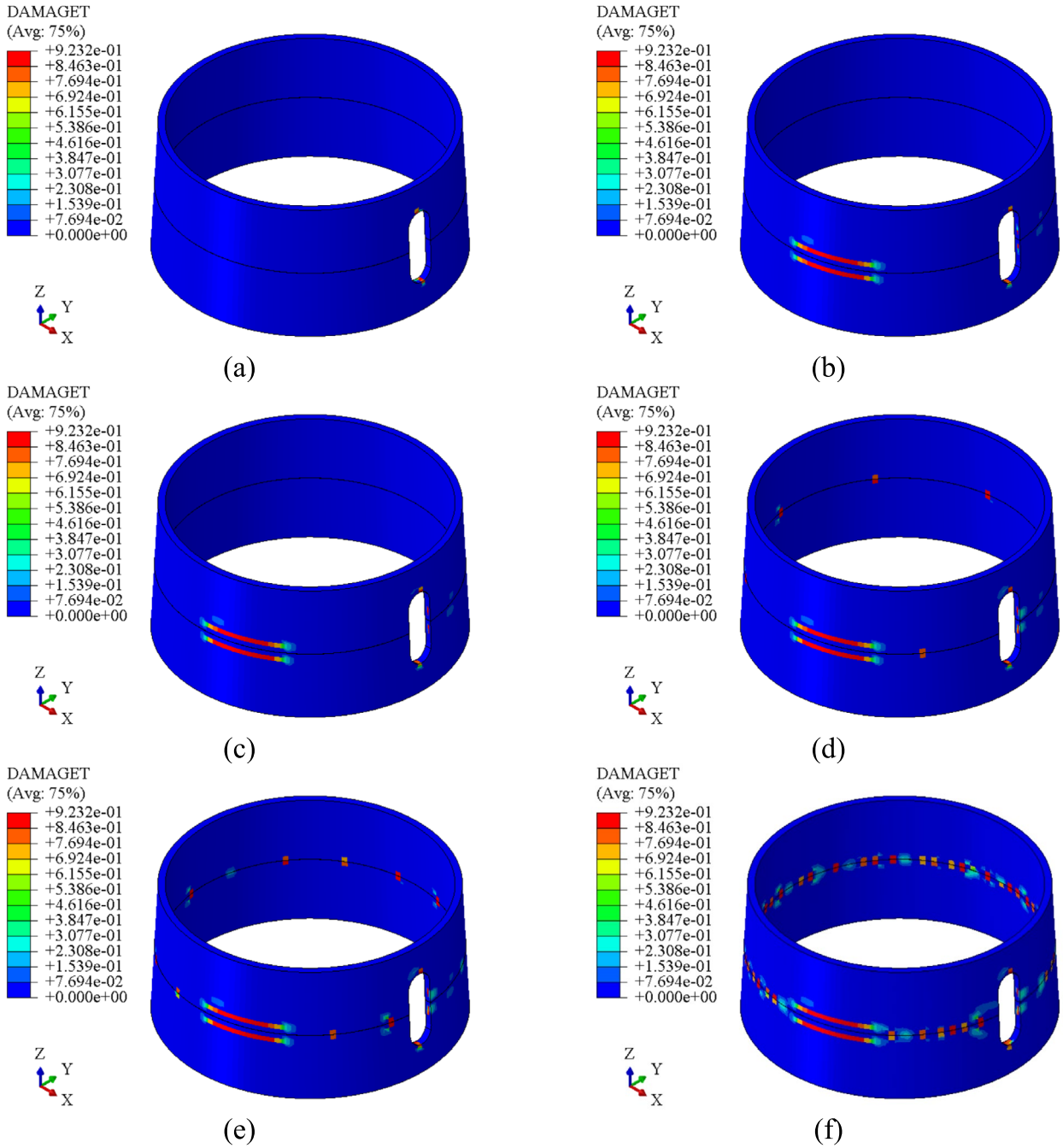


**Fig. 12** The tensile damage of concrete segments of model one for **a** case ideal, **b** case missing, **c** case filling, **d** case replacement one, **e** case replacement two, **f** case completion

representing the right side of the door and the rightmost representing the left side of the door. The Y-axis of the later figures represents the numerical value of stress (in MPa), with positive representing tensile stress and negative representing compressive stress.

#### *3.5.1 Model One*

As shown in Fig. 17, the surface contact stress line charts of Model One (no expansion grout) are presented. For Case Ideal, the entire section is in compressive stress and the value is even, with an increase near

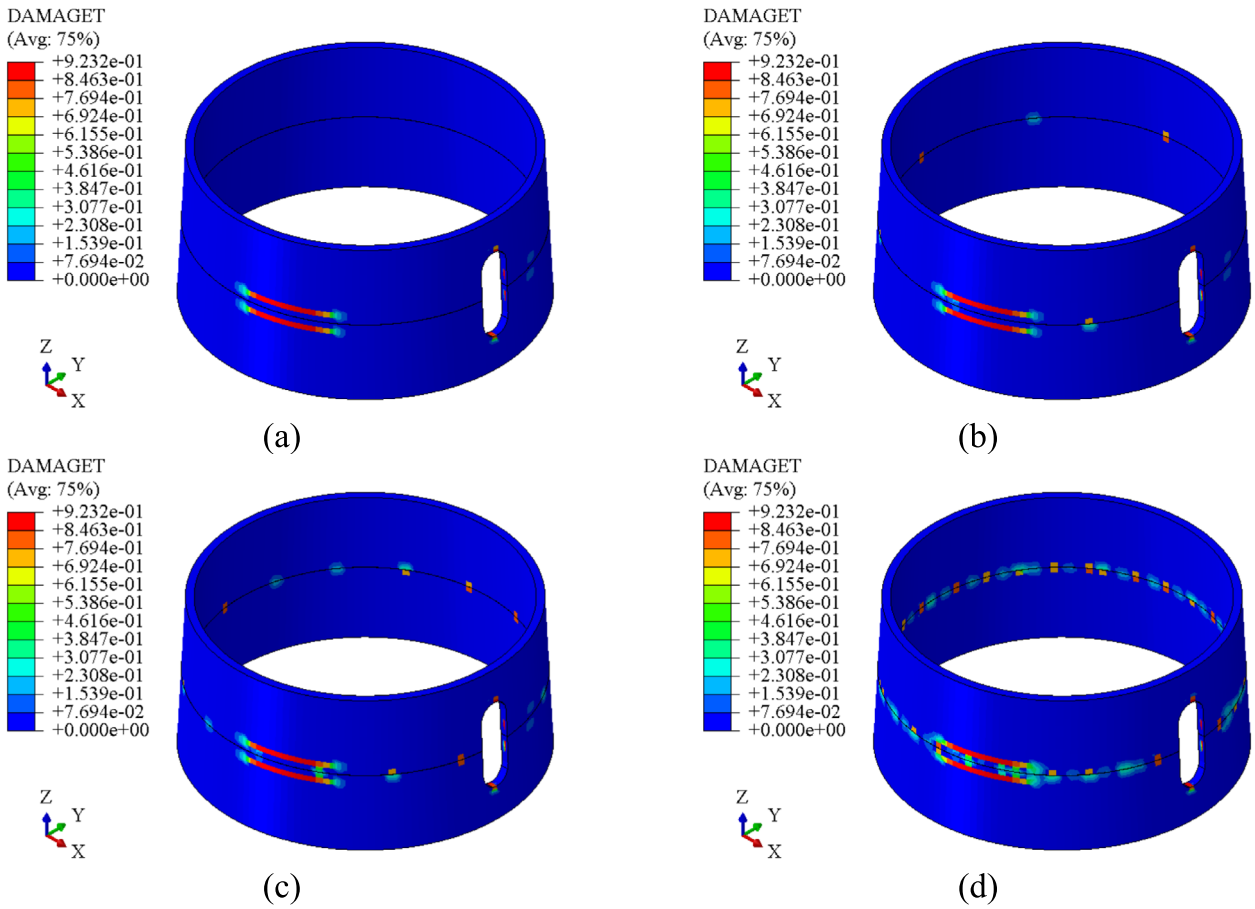


**Fig. 13** The tensile damage of concrete segments of model two for **a** case filling, **b** case replacement one, **c** case replacement two, **d** case completion

the door, and the compressive stress range is 5 to 17 MPa. The compressive stress values at Element 2 to 6 are generally around 12 MPa, which is in good agreement with the theoretical calculation value of 11.89 MPa considering the waterproof rubber and outer cavity, also validating the finite element model (Fig. 17a). For Case Missing, the stress distribution is significantly uneven and tensile stress appears in some areas, particularly in areas with serve grout missing. The maximum compressive stress is about 28 MPa and tensile stress is about 2 MPa (Fig. 17b). For Case Filling, the newly filled grout is subjected to less stress, so the overall contact stress is similar to that of Case Missing (Fig. 17c). For Case Replacement One and Two, the stress value corresponding to the grout chiseled area has a sudden change, with the extremum point showing tensile stress and both sides near the tensile point showing large compressive stress (Fig. 17d, e). For Case Completion, due to the fact that the newly filled grout cannot participate well in bearing load, the stress value fluctuates along the section position. The stress is mainly in compression, and the stress fluctuation near the door is relatively large (Fig. 17f).

#### *3.5.2 Model Two*

As shown in Fig. 18, the surface contact stress line charts of Model Two (slight expansion grout) are presented. There is no difference in the results between Model One and Model Two for Case Ideal and Case Missing (Fig. 17a, b). For Case Filling, assuming that the expansibility of newly filled grout can restore local deformation to the ideal state, the unevenness of stress is alleviated ideally (Fig. 18a). For Case Replacement One and Two, the stress corresponding to the grout chiseled area has a sudden change, with the extremum point showing tensile stress, while the repaired areas will restore to ideal stress values (Fig. 18b, c). For Case Completion, the stress tends to be even, and the entire section is in compressive stress. The overall stress distribution is similar to the Case Ideal, but with a slight fluctuation (Fig. 18d).

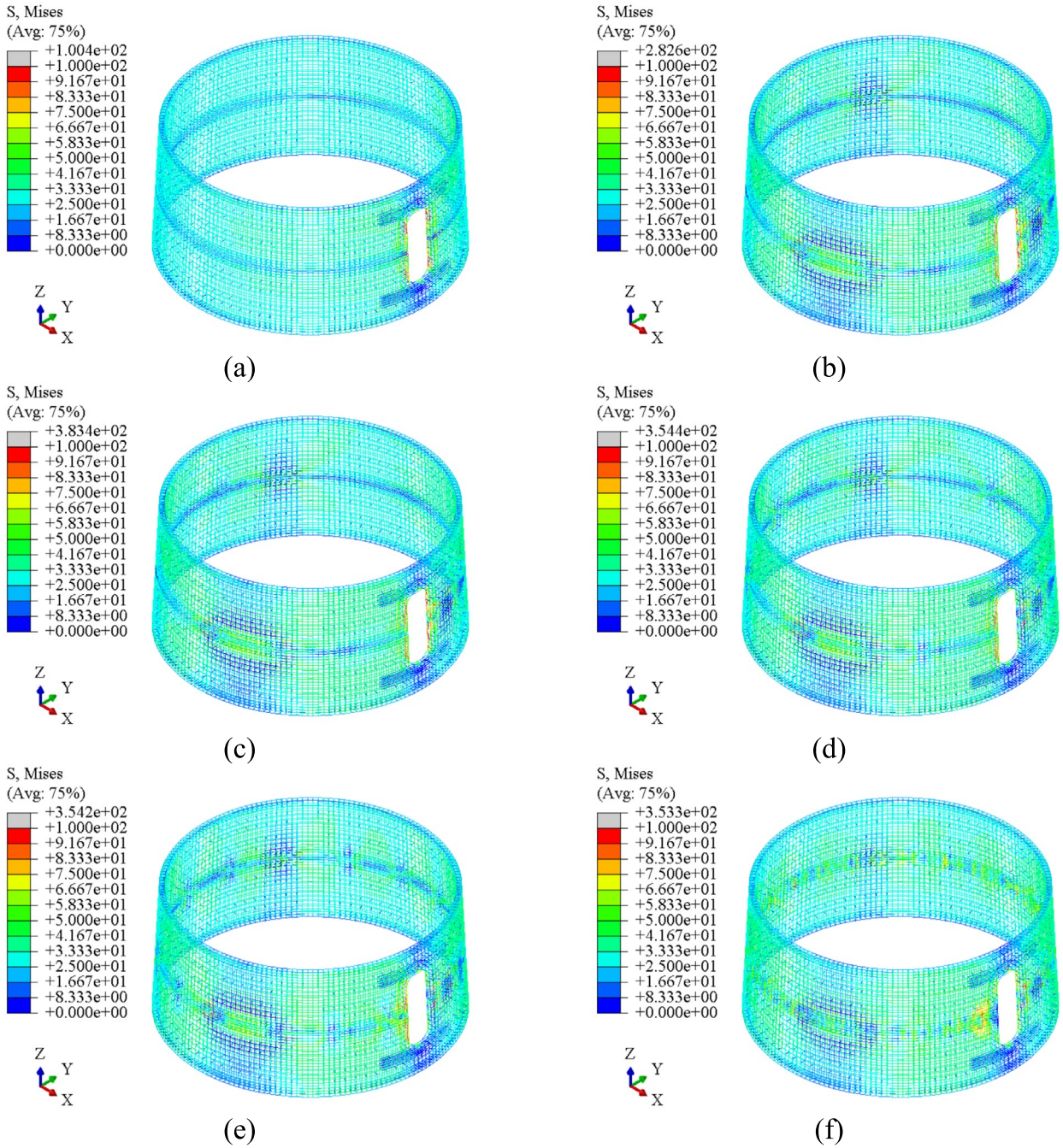


**Fig. 14** The mises stress of rebars of model one for **a** case ideal, **b** case missing, **c** case filling, **d** case replacement one, **e** case replacement two, **f** case completion

## 4 Fatigue Analysis

### 4.1 Method

The wind turbine prestressed concrete tower is subjected to fatigue loads up to millions of cycles during the service life. Although the stress range caused by these loads is generally not too large, such a big number of cycles may still make fatigue a control condition for tower design, especially when the concrete section has defects. Therefore, it is necessary to conduct the fatigue analysis and verification on concrete tower structures. Referring to Section 7.4.1 of the *fib Model Code for Concrete Structures 2010* (2013), this paper adopts the Palmgren-Miner summation method to calculate the fatigue damage factor ($D$) of the structure. If $D \leq 1.0$, it

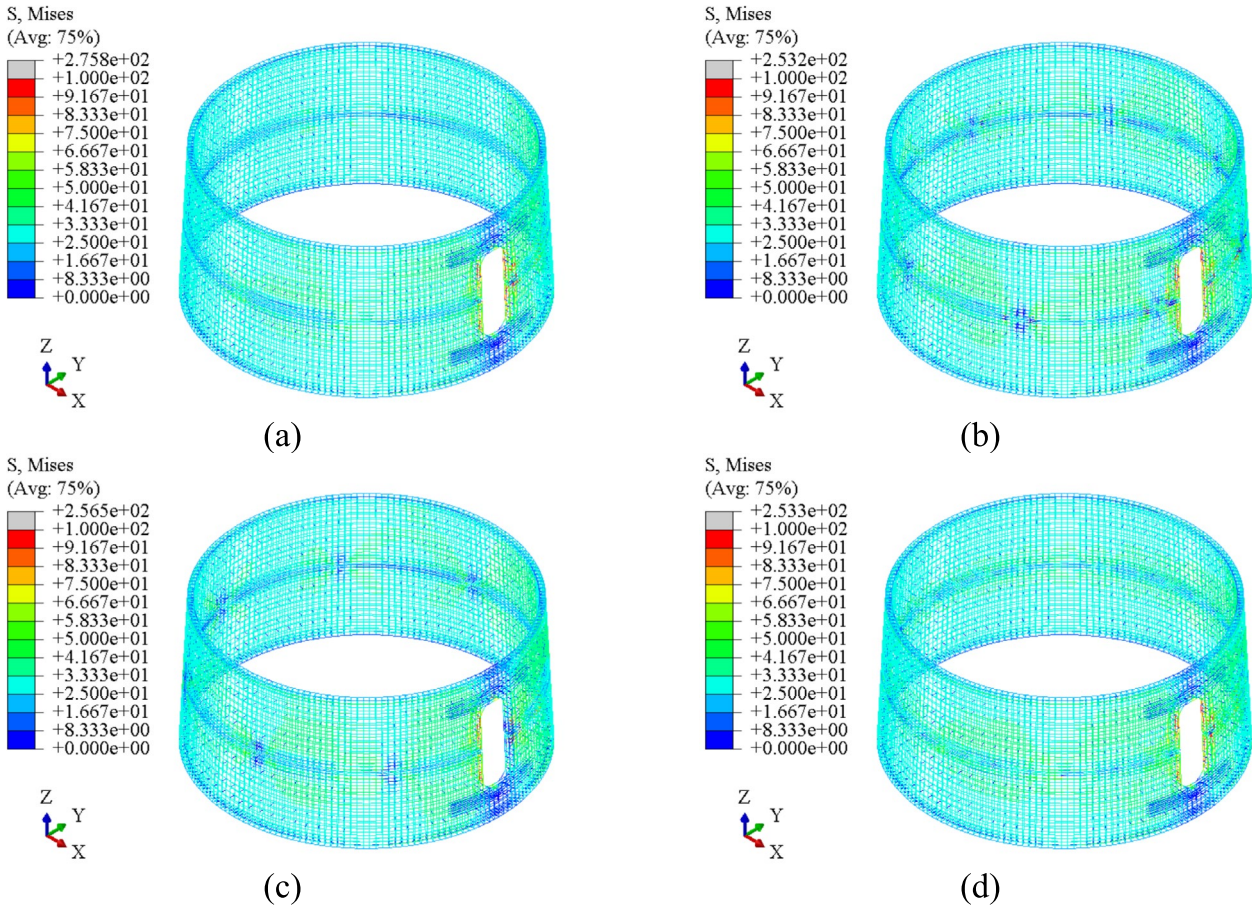


**Fig. 15** The Mises stress of rebars of model two for **a** case filling, **b** case replacement one, **c** case replacement two, **d** case completion

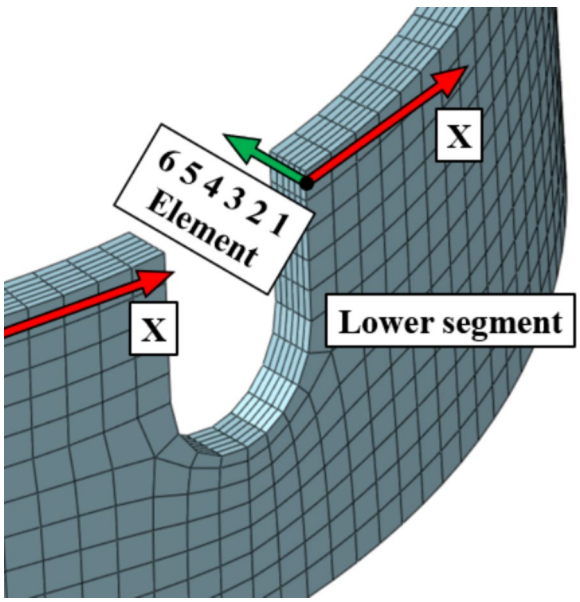


**Fig. 16** Segment contact surface

is considered to meet the fatigue design requirements (see Eq. (1)).

$$D = \sum_{i=1}^{j} \frac{n_{Ei}}{N_{Ri}} \leq 1.0 \tag{1}$$

where $n_{Ei}$ is the number of acting stress cycles associated with the actual stress levels for concrete; $N_{Ri}$ is the number of resisting stress cycles at a given stress level.

The $N_{Ri}$ of concrete needs to be calculated based on actual stress levels and stress range for concrete.

(1) When the two extreme stresses are both compression (see Eqs. (2)–(9)).

$$\log N_1 = \frac{8}{Y-1} \cdot (S_{cd,\max} - 1) \tag{2}$$

$$\log N_2 = 8 + \frac{8 \cdot \ln(10)}{Y-1} \cdot (Y - S_{cd,\min}) \cdot \log\left(\frac{S_{cd,\max} - S_{cd,\min}}{Y - S_{cd,\min}}\right) \tag{3}$$

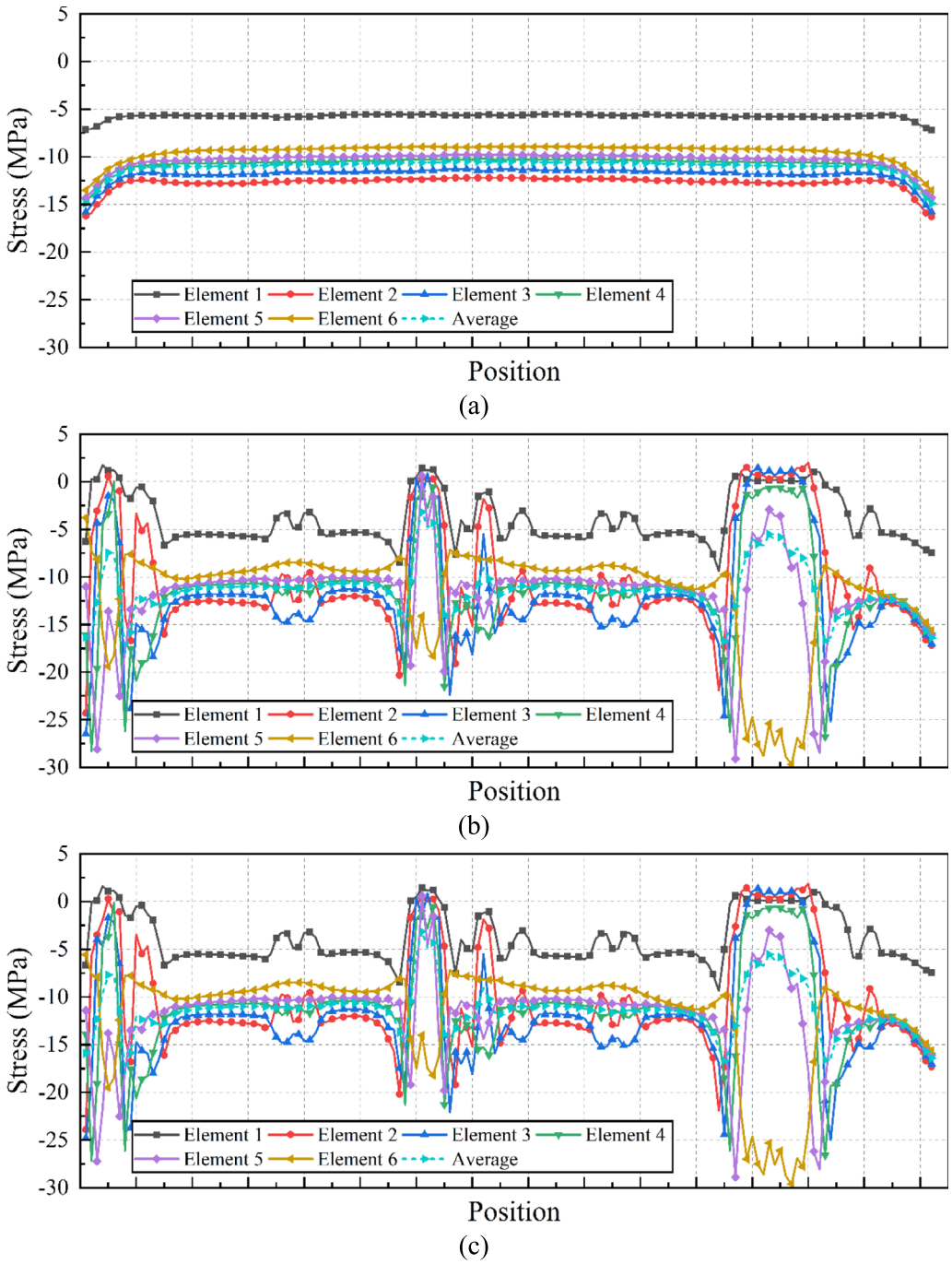


**Fig. 17** The contact stress of segment surface of model one for **a** case ideal, **b** case missing, **c** case filling, **d** case replacement one, **e** case replacement two, **f** case completion

$$\log N = \begin{cases} \log N_1 & (\log N_1 \le 8) \\ \log N_2 & (\log N_1 > 8) \end{cases} \tag{4}$$

where $S_{cd,\max}$ is the maximum compressive stress level; $S_{cd,\min}$ is the minimum compressive stress level, $N$ is the number of resisting stress cycles at a given stress level. The parameters can be calculated by following equations.

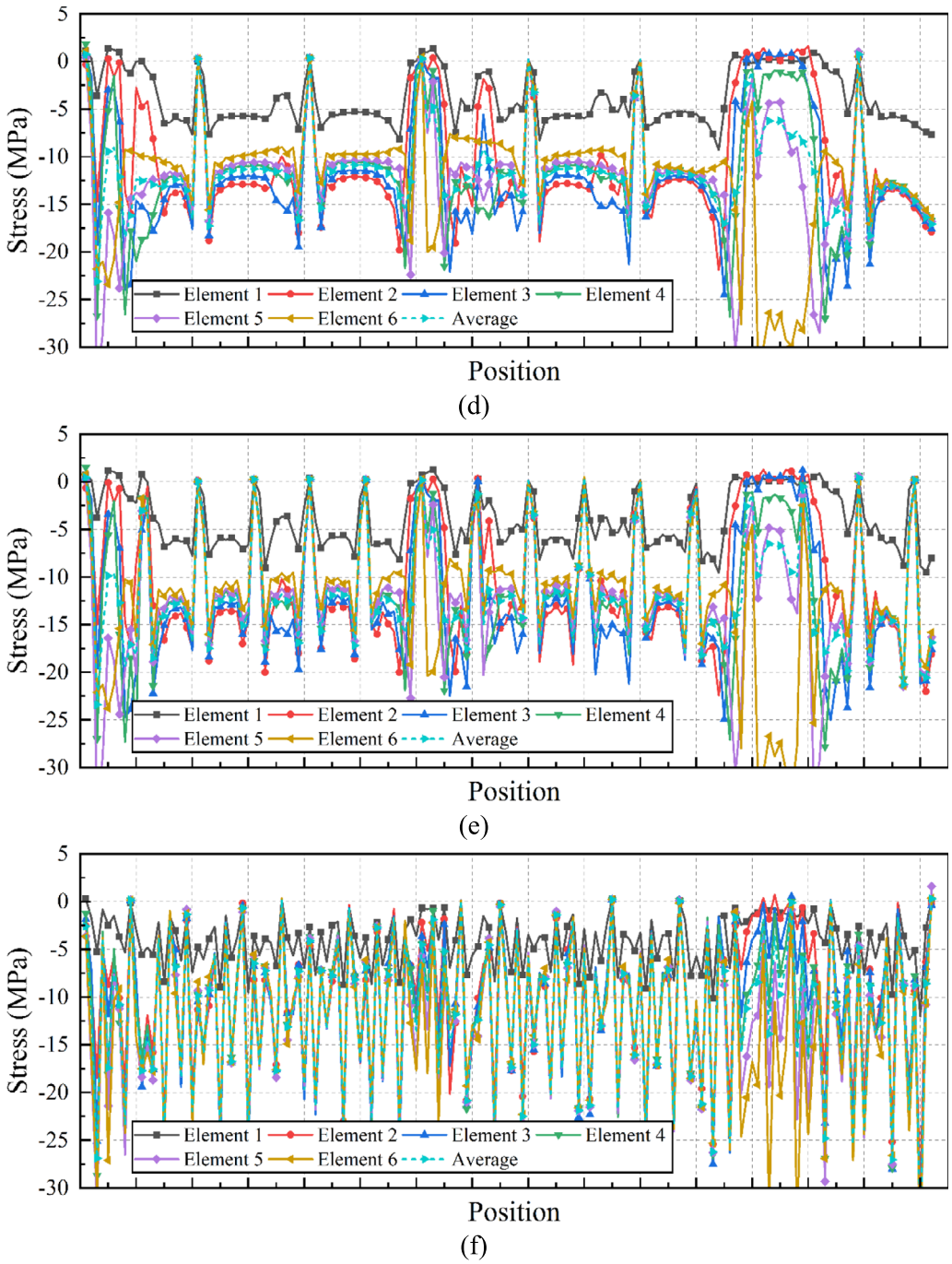


**Fig. 17** continued

$$Y = \frac{0.45 + 1.8 \cdot S_{cd,\min}}{1 + 1.8 \cdot S_{cd,\min} - 0.3 \cdot S_{cd,\min}^2} \tag{5}$$

$$S_{cd,\max} = \gamma_{Ed}\sigma_{c,\max}\eta_c / f_{cd,fat} \tag{6}$$

$$S_{cd,\min} = \min\{\gamma_{Ed}\sigma_{c,\min}\eta_c / f_{cd,fat},\ 0.8\} \tag{7}$$

$$f_{cd,fat} = 0.85 \cdot \beta_{cc}(t) \cdot f_{ck} \cdot \left(1 - \frac{f_{ck}}{400}\right) \Big/ \gamma_{c,fat} \tag{8}$$

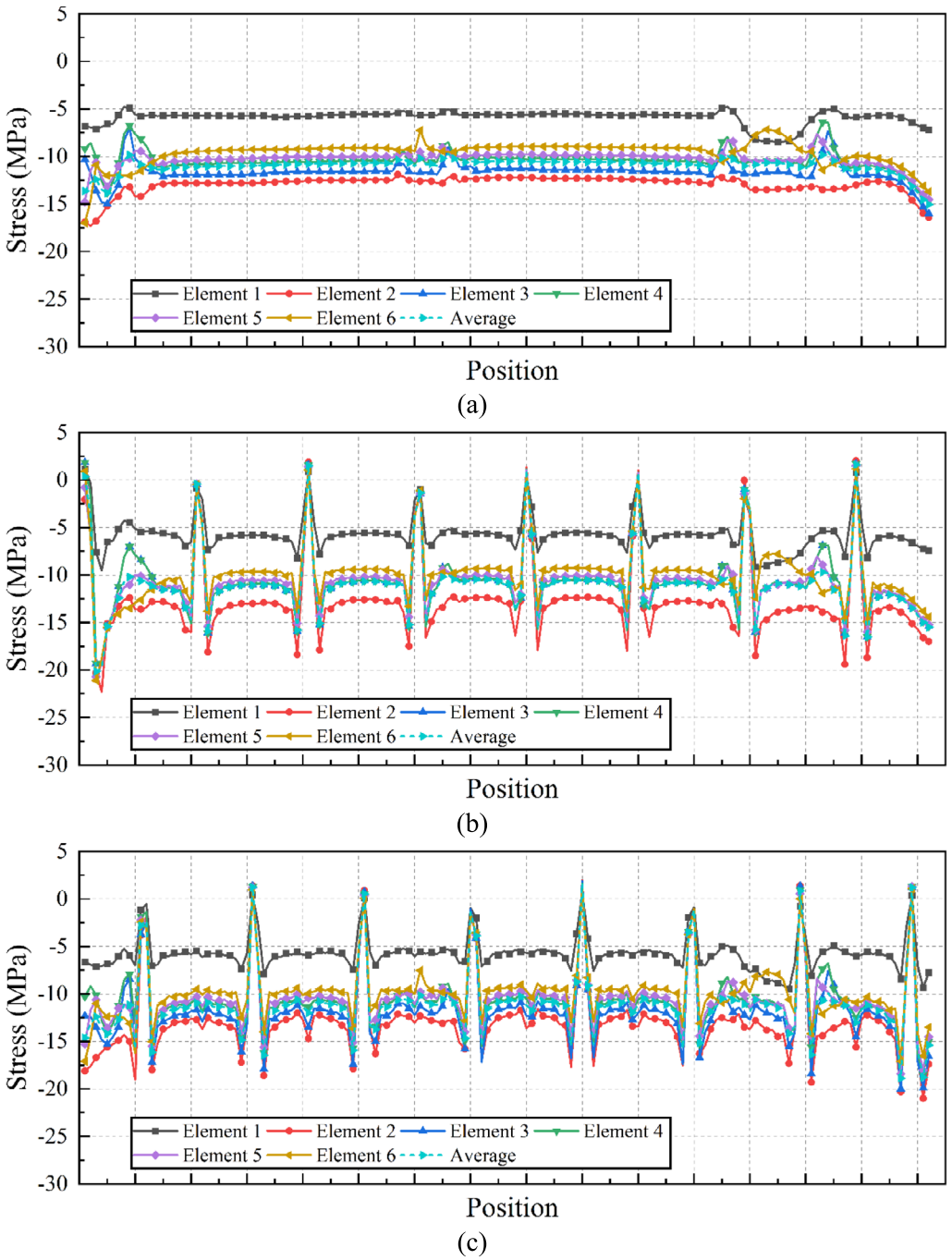


**Fig. 18** The contact stress of segment surface of model two for **a** case filling, **b** case replacement one, **c** case replacement two, **d** case completion

$$\beta_{cc}(t) = \exp\left\{s \cdot \left[1 - \left(\frac{28}{t}\right)^{0.5}\right]\right\} \tag{9}$$

where $\sigma_{c,\max}$ is the maximum compressive stress; $\sigma_{c,\min}$ is the minimum compressive stress; $\gamma_{Ed}$ is the load factor, taken as 1.1; $\eta_c$ is the averaging factor of concrete stresses in the compression zone considering the stress gradient, taken as 1.0; $\gamma_{c,fat}$ is the partial safety factor for concrete material properties under fatigue loading, taken as 1.5; $f_{ck}$ is the characteristic value of compressive strength of concrete, for C70 concrete in Chinese code taken as 55 MPa; $s$ is the coefficient which depends on the strength class of cement, taken as 0.2; $t$ is the concrete age in days adjusted, taken as 60 days.

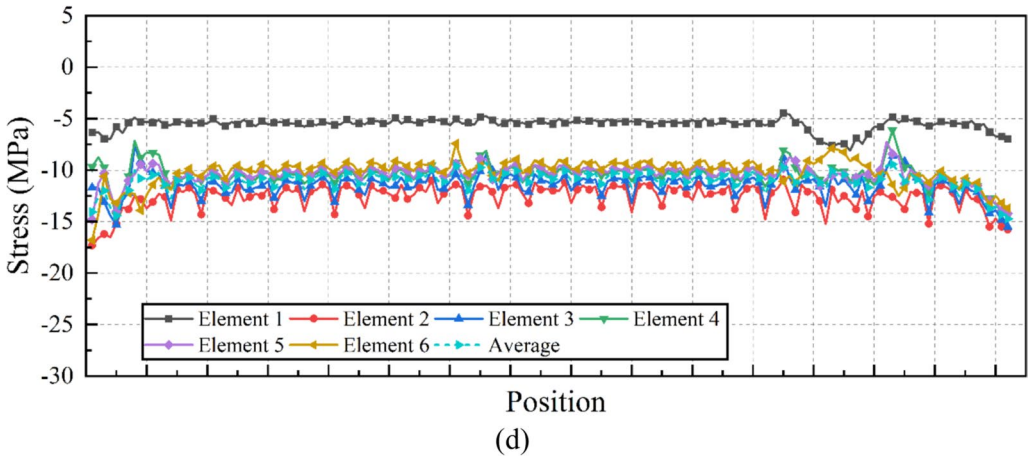


**Fig. 18** continued

(2) When the two extreme stresses are one compression and one tension with the condition $\sigma_{ct,\max} \leq 0.026|\sigma_{c,\max}|$ .

$$\log N = 9(1 - S_{cd,\max}) \tag{10}$$

(3) When the two extreme stresses are one compression and one tension with the condition $\sigma_{ct,\max} > 0.026|\sigma_{c,\max}|$, or the two extreme stresses are both tension (see Eqs. (11)–(13)).

$$\log N = 12(1 - S_{td,\max}) \tag{11}$$

$$S_{td,\max} = \gamma_{Ed} \cdot \sigma_{ct,\max} / f_{ctd,fat} \tag{12}$$

$$f_{ctd,fat} = f_{ctk,0.05} / \gamma_{c,fat} \tag{13}$$

where $S_{td,\max}$ is the maximum tensile stress level; $\sigma_{ct,\max}$ is the maximum tensile stress; $f_{ctk,0.05}$ is the characteristic value of 0.05 % proof axial tensile strength of concrete, for C70 concrete in Chinese code taken as 3.0 MPa.

Based on the above method, fatigue analysis and verification are conducted on the upper contact surface of the first tower segment. Considering a design service life of 20 years, the values and frequencies of the fatigue loads are calculated to obtain $n_{Ei}$. At the same time, considering the maximum bending moment as the control load, the stress levels and ranges of the concrete section are calculated to obtain $N_{Ri}$. Making a linear summation to calculate the fatigue damage factor ($D$) can make a verification to the target area of the concrete section.

### 4.2 Cases

The cases for fatigue verification are shown in Table 3. Among them, Case No.1 and No.2 take the theoretical calculation stress of ideal uniform compression distribution of the contact surface as the reference to calculate the stress level, and Case No.2 considers the section weakening of the waterproof rubber and outer cavity. The Initial cases in Table 3 correspond to the simulation cases in Table 2, which refers to using the stress of a certain simulation case to calculate the stress level for fatigue verification. For Case Ideal and Case Missing, the property of the grout has no impact on the analysis, since no repair process has been carried out. For Case Filling and Case Completion, the property of the grout is distinguished, with no expansion and slight expansion corresponding to Model One and Model Two (cf. Sect. 2.3), respectively. Specifically, this paper distinguishes whether the verification area is located near the tower door (Fig. 19). There is a significant stress concentration near the door even in Case Ideal (cf. Fig. 17a), which is not caused by the missing of grout. This adverse effect needs to be considered. Therefore, when setting the verification area near the door, the stress response under the load should be amplified to a certain extent. For the method of getting reference stress values, Single Point Extremum means directly using the extremum of a certain element from simulation results, and Thickness Average means using the arithmetic average of the stresses in Element 2 to 6 which have the grout layer to transfer the load. (cf. Sect. 3.4, Figs. 17).

### 4.3 Results

The fatigue verification results of various cases are shown in Table 4. Among them, Reference Stress means the stress of the concrete contact surface under the prestress of steel strands and the gravity of the upper tower, with positive values indicating tension and negative values indicating compression. The stress caused by external load is further calculated and added to Reference Stress.

**Table 3** Verification cases

| Number | Initial case | Grout property | Verification area | Method of getting value |
|---|---|---|---|---|
| 1 | – | – | Not near the door | Theoretical calculation with full cross-section |
| 2 | – | – | Not near the door | Theoretical calculation with the grout layer |
| 3 | Case ideal | – | Not near the door | Single point extremum |
| 4 | Case ideal | – | Near the door | Single point extremum |
| 5 | Case ideal | – | Not near the door | Thickness average |
| 6 | Case ideal | – | Near the door | Thickness average |
| 7 | Case missing | – | Not near the door | Single point extremum |
| 8 | Case missing | – | Near the door | Single point extremum |
| 9 | Case missing | – | Not near the door | Thickness average |
| 10 | Case missing | – | Near the door | Thickness average |
| 11 | Case filling | No expansion | Not near the door | Single point extremum |
| 12 | Case filling | No expansion | Near the door | Single point extremum |
| 13 | Case filling | No expansion | Not near the door | Thickness average |
| 14 | Case filling | No expansion | Near the door | Thickness average |
| 15 | Case completion | No expansion | Not near the door | Single point extremum |
| 16 | Case completion | No expansion | Near the door | Single point extremum |
| 17 | Case completion | No expansion | Not near the door | Thickness average |
| 18 | Case completion | No expansion | Near the door | Thickness average |
| 19 | Case filling | Slight expansion | Not near the door | Single point extremum |
| 20 | Case filling | Slight expansion | Near the door | Single point extremum |
| 21 | Case filling | Slight expansion | Not near the door | Thickness average |
| 22 | Case filling | Slight expansion | Near the door | Thickness average |
| 23 | Case completion | Slight expansion | Not near the door | Single point extremum |
| 24 | Case completion | Slight expansion | Near the door | Single point extremum |
| 25 | Case completion | Slight expansion | Not near the door | Thickness average |
| 26 | Case completion | Slight expansion | Near the door | Thickness average |

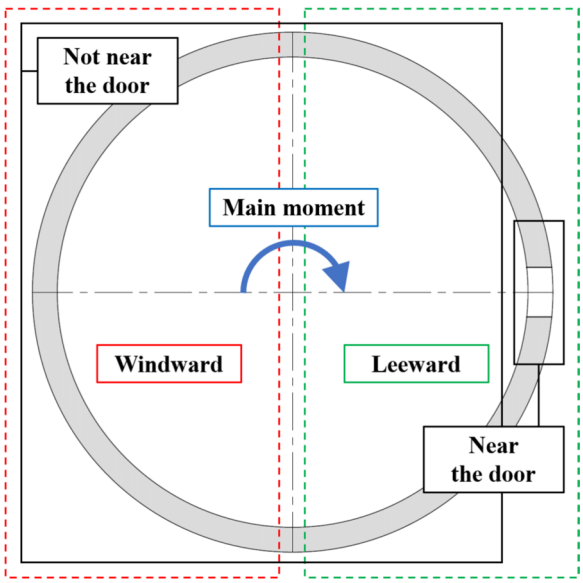


**Fig. 19** Fatigue verification area

The choosing of Reference Stress value is based on the worst condition, with the minimum compressive stress (or maximum tensile stress) taken for the windward verification and the maximum compressive stress taken for the leeward verification. The verification area can be windward or leeward, whether it is near the door or not (cf. Fig. 19). The damage factor ($D$) is defined as Eq. (1). When it is greater than 1.0, it indicates that the fatigue verification does not meet the requirements, and the font is bolded for easy observation in the table.

As shown in Table 4, the fatigue verifications for theoretical calculation (Case No.1 and No.2) and Case Ideal (Case No.3, No.4, No.5 and No.6) all meet the code requirements. The stress concentration of the door and method of getting reference stress value have no influence on the final results, it indicates the rationality of the tower section design. For Case Missing (Case No.7, No.8, No.9 and No.10), most of the fatigue verifications do not meet the requirements, and the damage factors significantly exceed the limit of 1.0, indicating that the uneven stress distribution caused by grout missing strongly weakens the fatigue performance of the local

**Table 4** Verification results

| Number | Reference stress (σ/MPa) | | Damage factor (*D*) | |
|---|---|---|---|---|
| | Windward | Leeward | Windward | Leeward |
| 1 | 9.95 | 9.95 | 5.29E−09 | 1.22E−08 |
| 2 | 11.89 | 11.89 | 1.37E−07 | 7.19E−07 |
| 3 | 8.93 | 16.30 | 9.65E−08 | 1.47E−05 |
| 4 | 10.40 | 16.30 | 6.62E−04 | 7.75E−03 |
| 5 | 10.50 | 14.88 | 1.08E−07 | 4.58E−06 |
| 6 | 11.50 | 14.88 | 8.32E−06 | 1.61E−03 |
| 7 | − 1.86 | 28.70 | **2.48E+43** | **2.58E+05** |
| 8 | − 1.60 | 28.30 | **8.43E+54** | **2.42E+09** |
| 9 | 3.34 | 17.81 | **5.82E+16** | 6.68E−05 |
| 10 | 7.45 | 16.40 | **3.81E+08** | 8.74E−03 |
| 11 | − 1.90 | 29.60 | **3.97E+43** | **2.71E+06** |
| 12 | − 0.28 | 27.20 | **1.47E+48** | **1.36E+08** |
| 13 | 3.15 | 17.97 | **5.47E+17** | 7.98E−05 |
| 14 | 7.64 | 16.42 | **4.05E+07** | 8.95E−03 |
| 15 | − 1.58 | 36.60 | **9.12E+41** | **2.39E+14** |
| 16 | − 1.58 | 36.60 | **6.66E+54** | **6.38E+18** |
| 17 | − 0.31 | 35.08 | **2.86E+35** | **4.50E+12** |
| 18 | − 0.31 | 35.08 | **2.09E+48** | **1.20E+17** |
| 19 | 6.39 | 17.30 | **1.40E+01** | 3.88E−05 |
| 20 | 7.63 | 17.30 | **4.56E+07** | 2.72E−02 |
| 21 | 9.52 | 15.06 | 9.87E−08 | 5.25E−06 |
| 22 | 10.30 | 15.06 | 6.45E−04 | 1.94E−03 |
| 23 | 6.11 | 17.30 | **3.80E+02** | 3.88E−05 |
| 24 | 7.15 | 17.30 | **1.31E+10** | 2.72E−02 |
| 25 | 9.26 | 14.72 | 9.74E−08 | 4.07E−06 |
| 26 | 10.01 | 14.72 | 4.37E−05 | 1.37E−03 |

The significance of bold indicates that the damage factor is greater than 1.0

concrete section. After the wind turbine running for a period of time under Case Missing, local fatigue failure of the concrete is likely to occur, and there is a potential risk to the whole structure of inclination or even collapse, so the repair is needed.

For Case Filling using no expansion grout (Case No.11, No.12, No.13 and No.14), the stress distribution is similar to that of the Case Missing, so the fatigue verification results are basically similar to those of the Case Missing. Most of the fatigue verifications do not meet the requirements, indicating that using no expansion grout for one-time filling repair is ineffective. For Case Completion (Case No.15, No.16, No.17 and No.18) using no expansion grout, the stress distribution of the section is shown in Fig. 17f. Due to the repair of chiseling and filling, the stress fluctuates along the section position, and the local high compressive or high tensile stress is unfavorable for the fatigue verification. The fatigue verifications of all cases do not meet the requirements, indicating that using no expansion grout for replacement repair cannot achieve the effect of improving the fatigue life of the structure.

For the Case Filling (Case No.19, No.20, No.21 and No.22) and Case Completion (Case No.23, No.24, No.25 and No.26) using slight expansion grout, the stress distribution tends to be even significantly compared with Case Missing, but the problem of local low compressive stress still exists (cf. Fig. 18a, d). This problem leads to a higher fatigue damage value on the windward side when using the Single Point Extremum method, which does not meet the verification requirements. However, when using the Thickness Average method, the fatigue damage on the windward side can meet the requirements. The fatigue verification on the leeward side meets the requirements, regardless of which method is used. It indicates that, while ensuring the construction quality, using slight expansion grout for one-time filling repair and replacement repair both can achieve an ideal result, remarkably decreasing the fatigue damage value and improving the fatigue life of the structure.

In addition, it is found that whether the fatigue verification area is located near the tower door or not is not a critical factor in whether the fatigue verification will meet the requirements or not. But the fatigue damage of the area not near the door is much smaller than that of the area near the door. Compared with the Single Point Extremum method, using the Thickness Average method homogenizes the local stress to some extent, so the calculated fatigue damage factor is smaller. Compared with using no expansion grout, using slight expansion grout can pronouncedly decrease the fatigue damage value and improve the fatigue life of the structure.

## 5 Conclusions

In this paper, a grout layer replacement repair scheme for grout missing in the horizontal joint of wind turbine prestressed concrete tower is proposed. Considering no expansion and of slight expansion grout, ABAQUS is used for finite element simulation of the horizontal joint replacement process. The concrete stress, tensile damage, contact surface stress, steel rebar stress and other responses of the concrete tower are obtained. Based on the simulation results, fatigue analysis is carried out on the concrete section near the horizontal joint. The potential risk caused by grout missing and the effectiveness of the grout layer replacement are revealed. The main conclusions are as follows.

(1) The grout layer missing in the horizontal joint has a significant adverse effect on the local area of the concrete tower. Based on the finite element simulation results, there is an obvious stress uneven-

ness in the local area of severe grout missing, with concrete compressive stress increasing or decreasing, tensile stress increasing, tensile damage zone developing, and steel rebars stress increasing or decreasing. This can lead to concrete cracking and blocks falling. Based on the fatigue analysis results, the fatigue damage factor greatly exceeds the limit value for the case of grout layer missing, meaning a short fatigue life. In this situation, there is a risk to the structure of local failure and repair of the grout layer is required.

(2) The repair of the grout layer for the horizontal joint should use slight expansion grout (whose expansibility should be able to restore the local deformation to the ideal state), or adopt measures such as local lifting to promote stress redistribution, so that the grout layer can immediately participate in bearing load after repair. Based on the simulation results, the effectiveness of slight expansion grout is much better than that of no expansion grout, and the concrete stress, surface contact stress, and steel rebars stress tend to be more even. The concrete tensile damage develops during the replacement process, and there is no noticeable difference between using two types of grouts. Based on the fatigue analysis results, the effectiveness of slight expansion grout is also much better. The fatigue damage factors for the cases of grout filling and replacement completion are significantly decreased, that is, the fatigue life is improved. In this situation, the fatigue damage factors can generally meet the requirements.

This paper conducts numerical simulation and fatigue analysis research on the replacement of grout layer for horizontal joint of wind turbine prestressed concrete tower, in order to provide theoretical and technical support for the analysis and solution of similar grout missing problems and grout layer replacement projects.

**Acknowledgements**
The authors gratefully acknowledge the support from National Key Research and Development Program of China (2024YFF0505400) and Fundamental Research Funds for the Central Universities.

**Author contributions**
Ziwei Wang: Methodology, Formal analysis, Investigation, Writing—Original Draft, Visualization. Dongping Huang: Investigation, Resources. Minjuan He: Conceptualization, Supervision. Zheng Li: Writing—Review and Editing, Funding acquisition, Project administration.

**Funding**
(1) National Key Research and Development Program of China (2024YFF0505400). (2) Fundamental Research Funds for the Central Universities.

**Data availability**
Data will be made available on request.

## Declarations

**Ethics approval and consent to participate**
Not applicable.

**Consent for publication**
Not applicable.

**Competing interests**
The authors declare that they have no known competing financial interests or personal relationships that could have appeared to influence the work reported in this paper.

Received: 7 January 2025 Accepted: 6 May 2025
Published online: 26 August 2025

**References**

Alvarez-Anton, L., Koob, M., Diaz, J., & Minnert, J. (2016). Optimization of a hybrid tower for onshore wind turbines by Building Information Modeling and prefabrication techniques. *Visualization in Engineering, 4*(1), 3. https://doi.org/10.1186/s40327-015-0032-4

Cao, Y., He, M., Ma, R., Yang, R., & Liang, F. (2020). Beam-column modeling and seismic fragility analysis of a prestressed segmental concrete tower for wind turbines. *Advances in Structural Engineering, 23*(8), 1715–1727. https://doi.org/10.1177/1369433219900295

Chen, J., Lin, W., & Li, J. (2024b). Ultimate torsional moment of dry horizontal joint for prefabricated concrete tower. The Structural Design of Tall and Special Buildings, e2156. https://doi.org/10.1002/tal.2156

Chen, J., Zhao, S., Zhang, Y., Tan, X., & Zhang, B. (2024a). Axial compressive performance of composite cylinder wall members in steel-concrete towers designed for wind turbines. *Journal of Constructional Steel Research, 221*, Article 108908. https://doi.org/10.1016/j.jcsr.2024.108908

Cheng, Y., Zhao, Y., Qi, H., & Zhou, X. (2024). Intelligent optimal design of steel-concrete hybrid wind turbine tower based on evolutionary algorithm. *Journal of Constructional Steel Research, 218*, Article 108729. https://doi.org/10.1016/j.jcsr.2024.108729

DNVGL-ST-0126 Support structures for wind turbines. (2016). DNV.

Elruby, A. Y., & Nakhla, S. (2019). Strain energy density based damage initiation in heavily cross-linked epoxy using XFEM. *Theoretical and Applied Fracture Mechanics, 103*, Article 102254. https://doi.org/10.1016/j.tafmec.2019.102254

fib Model Code for Concrete Structures 2010. (2013). John Wiley & Sons, Ltd.

Fürll, F., Klein, F., Hartwig, S., Kang, C., Betz, T., & Marx, S. (2024). Experimental and analytical study on the load-bearing capacity of segmented tower structures with dry joints under combined loading. *Structural Concrete*. https://doi.org/10.1002/suco.202300873

GB 50010-2010 Code for Design of Concrete Structures. (2015). China Architecture & Building Press.

Grünberg, J. & Göhlmann, J. (2013). Concrete structures for wind turbines. John Wiley & Sons, Ltd. https://doi.org/10.1002/9783433603291

GWEC. (2024). Global Wind Report 2024.

Hernandez-Estrada, E., Lastres-Danguillecourt, O., Robles-Ocampo, J. B., Lopez-Lopez, A., Sevilla-Camacho, P. Y., Perez-Sariñana, B. Y., & Dorrego-Portela, J. R. (2021). Considerations for the structural analysis and design of wind turbine towers: A review. *Renewable and Sustainable Energy Reviews, 137*, Article 110447. https://doi.org/10.1016/j.rser.2020.110447

IEC 61400-1:2019 Wind energy generation systems Part 1: Design requirements. (2019). International Electrotechnical Commission.

IEC 61400-6:2020 Wind energy generation systems Part 6: Tower and foundation design requirements. (2020). International Electrotechnical Commission.

Iwamoto, T., Nagai, T., & Sawa, T. (2010). Experimental and computational investigations on strain rate sensitivity and deformation behavior of bulk materials made of epoxy resin structural adhesive. *International Journal of Solids and Structures, 47*(2), 175–185. https://doi.org/10.1016/j.ijsolstr.2009.09.026

Jonscher, C., Liesecke, L., Penner, N., Hofmeister, B., Grießmann, T., & Rolfes, R. (2023). Influence of system changes on closely spaced modes of a large-scale concrete tower for the application to structural health monitoring. *Journal of Civil Structural Health Monitoring, 13*(4), 1043–1060. https://doi.org/10.1007/s13349-023-00693-6

Kang, C., Hartwig, S., & Marx, S. (2019). Behavior of externally prestressed segmental towers' dry joint under torsion effects. *Structural Concrete, 20*, 1350–1357. https://doi.org/10.1002/suco.201800266

Klein, F., Fürll, F., Betz, T., & Marx, S. (2022). Experimental study on the joint bearing behavior of segmented tower structures subjected to normal and bending shear loads. *Structural Concrete, 23*, 1370–1384. https://doi.org/10.1002/suco.202100710

LaNier, M. W. (2005). LWST phase i project conceptual design study: evaluation of design and construction approaches for economical hybrid steel/concrete wind turbine towers; June 28, 2002–July 31, 2004 (NREL/SR-500-36777). *NREL*. https://doi.org/10.2172/15011444

Li, Z., Xu, B., & Zhao, Y. (2024). Two-scale probabilistic seismic fragility assessment for a prestressed concrete-steel hybrid wind turbine tower with incremental dynamic and multiple stripe analysis. *Journal of Earthquake Engineering, 28*(14), 4025–4046. https://doi.org/10.1080/13632469.2024.2361770

Lin, L., Zhang, X., Zhang, D., Wu, X., Liu, Y., Wang, X., Wang, H., Wang, F., & Yang, T. (2023). Damage evolution and failure analysis of the advanced transition segment behavior of wind turbine tower. *Engineering Failure Analysis, 152*, Article 107527. https://doi.org/10.1016/j.engfailanal.2023.107527

Lotfy, I. (2012). Prestressed Concrete Wind Turbine Supporting System [University of Nebraska - Lincoln].

Ma, H., Zhang, D., Ma, Z., & Ma, Q. (2015). Scale model experimental of a prestressed concrete wind turbine tower. *Wind and Structures, 21*(3), 353–367. https://doi.org/10.12989/was.2015.21.3.353

Pang, B., Zhang, Y., & Liu, G. (2018). Study on the effect of waterborne epoxy resins on the performance and microstructure of cement paste. *Construction and Building Materials, 167*, 831–845. https://doi.org/10.1016/j.conbuildmat.2018.02.096

Peggar, R. (2017). Design and structural testing of tall Hexcrete wind turbine towers [Iowa State University].

Ren, W., Deng, R., Zhou, X., Wang, Y., Cao, F., & Jin, K. (2023). Compressive behavior of the steel–concrete composite adapter for wind turbine hybrid towers. *Engineering Structures, 280*, Article 115703. https://doi.org/10.1016/j.engstruct.2023.115703

Sidoroff, F. (1981). Description of Anisotropic Damage Application to Elasticity. Physical Non-Linearities in Structural Analysis (pp. 237-244). Springer Berlin Heidelberg. https://doi.org/10.1007/978-3-642-81582-9_35

Song, H., Cong, O., Hao, H., & Xu, Y. (2016). Research on mechanical behaviors of horizontal joint connection of prefabricated concrete towers. *Building Structure, 46*, 16–20.

Tao, Z., Wang, Z., & Yu, Q. (2013). Finite element modelling of concrete-filled steel stub columns under axial compression. *Journal of Constructional Steel Research, 89*, 121–131. https://doi.org/10.1016/j.jcsr.2013.07.001

von der Haar, C., & Marx, S. (2015). Design aspects of concrete towers for wind turbines. *Journal of the South African Institution of Civil Engineering, 57*(4), 30–37. https://doi.org/10.17159/2309-8775/2015/v57n4a4

## Publisher's Note



**Ziwei Wang** is a PhD candidate in College of Civil Engineering at Tongji University.

**Dongping Huang** is a Senior Engineer in Tongji Architectural Design (Group) Co., Ltd.

**Minjuan He** is a Professor in College of Civil Engineering at Tongji University.

**Zheng Li** is a Professor in College of Civil Engineering at Tongji University.